IMPROVEMENT OF INSULATION OF REENTRY VEHICLE

A thesis submitted in partial fulfilment of the requirements for the award of degree of

B.Tech

In

MECHANICAL ENGINEERING

By

FASIL K M (15120418)
SAYUJ S (15120447)
SREEJIN P S (15120452)
SREEJU C NAIR (15120454)
VENKATADAS M MALLAYA (15120456)

DEPARTMENT OF MECHANICAL ENGINEERING

COLLEGE OF ENGINEERING ADOOR

MANAKALA-691551

APRIL 2015

BONAFIDE CERTIFICATE

This is to certify that the project titled **IMPROVEMENT OF INSULATION OF REENTRY VEHICLE** is a bonafide record of the work done by

FASIL K M (15120418)
SAYUJ S (15120447)
SREEJIN P S (15120452)
SREEJU C NAIR (15120454)
VENKATADAS M MALLAYA (15120456)

In partial fulfilment of the requirements for the award of the degree of **BACHELOR OF TECHNOLOGY** in specialisation of **COCHIN UNIVERSITY AND SCIENCE AND TECHNOLOGY at COLLEGE OF ENGINEERING ADOOR, MANAKKALA**, during the year 2014 - 2015 .

Mr MANU M JOHN | **Mr MANU M JOHN**

GUIDE | **HEAD OF DEPARTMENT**

Project viva –voce held on --

INTERNAL EXAMINER | **EXTERNAL EXAMINER**

ABSTRACT

Hypersonic vehicles have to withstand extremely high aerodynamic heating and pressure loads during the ascent and re-entry stages. Multilayer thermal insulations have been widely designed in thermal protection systems to keep the temperature of underlying structure within an acceptable limit. In this study, a theoretical model is built combining radiation and conduction heat transfer in high temperature multilayer insulations under aerodynamic heating conditions. After a reliable validation with previous references, the effects of the layout, the number and the location of the foils, the density of insulation materials and the emissivity of the surface of foils on the insulation performance of multilayer thermal insulations are investigated, respectively. It is found that there exist an optimal number of insulation layers for best thermal performance and the layout of radiation foils has no evident effect. In addition, the insulation performance is much better when the foils are near the cold boundary, and when the density of insulation material and the emissivity of the surface of foils are higher, the temperature of bottom surface is lower**.**

ACKNOWLEDGEMENT

At the outset, I thank the lord almighty for the grace, strength and hope to make my endeavour a success.

I express my gratitude to **Mr Manu M John** HOD Mechanical Department, Project Guide and **Mr Venkitaraj K P**, Project Coordinator for providing me with adequate facilities, ways and the means by which I was able to complete my project. I express my sincere gratitude towards them for their constant support and valuable suggestions without which the successful completion of the project would not have been possible. I specially thank **Mr Manu M John** Project Guide and HOD Mechanical Engineering Department for allowing us to use the resources from Computational Fluid Dynamics Lab

I thank all my friends and family members who in one way or the other helped me in the successful completion of my work.

FASIL K M (15120418)
SAYUJ S (15120447)
SREEJIN P S (15120452)
SREEJU C NAIR (15120454)
VENKATADAS M MALLAYA (15120456)

TABLE OF CONTENTS

LIST OF FIGURES

LIST OF TABLES

CHAPTER 1

INTRODUCTION

During re-entry, in order to slow down the speed of space vehicles approaching the planet, space vehicles are forced to withstand Aerodynamic heating ranging from 377^{o}C to 1400^{o}C. Thus, a Thermal protection system (TPS) is utilized to maintain the underlying Structural temperature of a reusable launch vehicle within acceptable limits. It is required that a TPS should be extremely efficient and performs the task of thermal protection/insulation perfectly. TPS is divided into three categories: passive, semi-passive and active TPSs [1]. Among them, passive ones are characterized as the safest and lightest [6]. Multilayer thermal protection system is one of the most weight-efficient among all passive TPSs. Therefore it has a great potential for thermal protection and insulation, and is commonly applied into high temperature and cryogenic situations, e.g., [3].Multilayer thermal insulations are often designed in thermal protection systems to keep the temperature of underlying structure within an acceptable limit and satisfy the requirement of mechanical loads. For example, Daryabeigi [7] developed a numerical model for modelling combined radiation/conduction heat transfer in high-temperature multilayer insulation and validated it by comparing with experimental results. He found that when the foil spacing was 2mmand the foils were located near the hot boundary (the top foil was 2mmaway from the hot boundary), the insulation design was the most effective.

During hypersonic vehicles re-entry into the atmosphere, a multilayer insulation consists of combined heat transfer modes including radiation, solid conduction through fibrous, gas conduction and natural convection. However, natural convection and gas conduction are ignored here. The combined radiation/conduction heat transfer in high-temperature multilayer insulation is investigated in the present study. The multilayer insulation is composed of fibrous insulation spacers, which is separated by thin ceramic/ composite foils with gold coatings of high reflectance. The objective of this study is to investigate the effects of the number of fibrous insulation layers, the layout, number of the foils, the density of insulation material and the emissivity of reflective foil on the thermal insulation through the multilayer insulations. A finite element analysis is used to build a theoretical model combining radiation and conduction heat transfer in high temperature multilayer insulations under aerodynamic heating conditions and analyse effects of the above variables on the multilayer insulations.

Multilayer insulation consists of reflecting screen of high reflective index and spacers of low thermal conductivity arranged alternatively, whose insulation ability is better than any conventional insulation. Metal foil is usually used as reflecting screen in high temperature station and resisting heat flow into the inside structure. Metallic TPS consists of metallic shell panel fabricated from high temperature alloy and mechanically attached to the substructure. Heat transfer through the insulation involves combined modes of heat transfer: solid conduction through fibres, gas conduction and natural convection in the space between fibres and radiation through participating media which includes absorption, scattering and emission of radiant energy by the fibres. The relative contributions of the different heat transfer modes vary during re-entry. Radiation becomes more dominant at high temperatures with large temperature differences through the insulation, while gas conduction and natural convection contributions are minimal at low pressures and become more significant with increasing pressures. MLI designs typically rely on using a significant number of closely spaced thin reflecting foils separated by either thin fibrous insulation fibres or by using integral spacers such as crinkling or dimpling the foils. In most designs spacers are simply used to ensure various foils don’t touch each other, maintain the desired spacing between the foils.

The radiation heat transfer between successive highly reflective foils then provides the necessary thermal resistance to transfer heat through these MLI. The principle behind MLI is radiation and conduction balance. The layers of MLI can be arbitrarily closed to each other as long as they are not in thermal contact. To reduce weight and blanket thickness, the internal layers are made very thin and they need to be opaque. MLI consists of mainly two components: 1) reflective foils, 2) insulation spacers. Reflective foils are used to reduce the radiation component during re-entry heating and thus increases the radiative heat transfer.

CHAPTER 2
LITERATURE REVIEW

The heat transfer through multilayer insulation involves the combined modes of conduction and radiation. Over the years a number of studies were carried out to build a mathematical model and to study the performance of high temperature multilayer insulation.

2.1 COMPUTATIONAL, NUMERICAL AND EXPERIMENTAL STUDIES

A numerical model of the combined conduction and radiation heat transfer in high temperature multilayer insulation was modelled using finite volume method. The effective thermal conductivity of the MLI sample was calculated numerically. A steady state transient experiment were conducted and effective thermal conductivity was measured over an extended temperature and pressure range of 373 K to 1273 K and 1 x 10^{-4} to 760 mm of Hg. The numerical model was validated by comparison with steady – state effective thermal conductivity measurements, and by transient thermal tests simulating re-entry aerodynamic heating conditions. The two flux radiation modelling with isotropic scattering was used to model radiation, and optimized the location of reflective foils throughout the insulation. *Kamran Dariyabeigi [1]*.

Experimental and theoretical studies were carried out for the determination of the effective thermal conductivities of multilayer thermal insulations system with specially designed shields for the determination of the effective thermal conductivities of multilayer thermal insulation systems with specially designed shields for application in high temperature fuel cells. A theoretical model based on combined conduction and radiation heat transfer through porous material capable of absorbing, emitting and scattering has been used to predict the temperature distribution and heat transfer in insulations comprised of the materials separated by multiple screens (shields). The experimental results obtained for several multilayer thermal insulation systems are reported, and the experimental data are compared with theoretical predictions to assess the effectiveness of the screens in reducing the effective thermal conductivity of the insulations and the lowest thermal conductivity were achieved with micro porous materials. *(Markus spinnler, Edgar R.F. Winter and Raymond Viskanta [6]*.

Later a theoretical model of high temperature multilayer insulation was prepared with the help of the finite volume method. The parameters were calculated using the inverse problem method. The equivalent radiation transmittance, absorptivity, reflectivity were used to investigate the radiation heat transfer and a linear function to describe the relationship between the temperature and conductivity of the solid and gas. Comparisons, with deviations less than 4% were carried out between the predicted effective thermal conductivities and the measured ones in high temperature insulation and the deviations of comparisons between the predicted transient temperature variations and the measured ones are less than 6.5% at the depth of 5mmin multilayer thermal insulation. The results confirm the validity of results and good behaviour of the theoretical model *(Huang Cam, Zhang Yue [3])*.

The applicability of carbon – based foams as an insulation material in the thermal protection systems (TPSs) of space vehicles considered using a physical analysis and computer modelling. The heat transfer through the foam is considered in its solid phase and the gas residing in the foam is considered in its solid phase and the gas residing in the foam pores via conduction and radiation. As the cellular structure of the foam prevents a large scale motion of the gas, the convection is neglected as a heat transfer mode. The results obtained show that the gas phase conduction and radiation can be ignored and at near room temperatures and at sub atmospheric pressures but their contributions at high temperatures and at atmospheric pressure become very significant.

It is also found that we can derive an analytical expression for the effective thermal conductivity (a parameter that combines both conduction and radiation) as a function of temperature and pressure. Such an expression is found to be valid for quite a large range of temperature, pressure and insulation thickness and, due to its mathematical simplicity, is very suitable for use in computationally intensive large-scale thermo-mechanical analysis of the entire TPS of a space vehicle (M *Grujicic, C L Zhao, S B Biggers, J M Kennedy, and D R Morgan[9])*

Spacer material used in the insulation is changed and the study was conducted by preparing a new kind of MLI in which the spacer material was made from Al_2O_3 fibre mat and silica aero gels is implanted on the surface of Al_2O_3 fibre through sol-gel process. In high vacuum the effective thermal conductivity is reduced by 21.8% and weight by 67.2 %. This new kind of material shows good insulation performance in high temperature of 1200K and low vacuum. The reflective foil used in a multilayer insulation is of two types , the first one is a reflective screen made of reflective foil and is used in high temperature conditions and the second type is the screen made of metallic plating film used in low temperature conditions . Perforations are considered in the spacer material as it helps in reducing the effect of gaseous conduction. Hence the heat transfer is different when compared to other insulation materials.

The effect of layer density and screen emissivity on the thermal characteristics of the MLI such as the effective thermal conductivity and heat flux is studied. It was observed that the effective conductivity and heat flux increases with increase of emissivity of reflective screen. As the layer density of the material increases the effective conductivity and heat flux across the insulation decreases even if emissivity is increases (*Peng Li, Huier Cheng [4]).*

In order to find the effective thermal conductivity various analytical methods were developed and one such numerical model was developed. Effective thermal conductivities of the fibrous insulation were measured over wide temperature ranges. The optically thick assumption was used to describe the radiation heat transfer through the insulation. Solid and radiative contributions in the insulation are found to be independent of pressure. (*Shu-yuan Zhao, Bo-ming Zhang, Xiao-dong He [7])*

CHAPTER 3

PHYSICAL MODEL

Fig.3.1 schematically shows a multilayer insulation sample used to validate the presented numerical heat transfer model. The multilayer structure consists of six layers of fibrous insulation spacers, which are separated by five reflective foils with an emissivity of 0.02. Note that the total number of insulation layers (N) is always one more than the total number of reflective foils (N _ 1).The entire thickness of the multilayer insulation sample is 20 mm. The thickness of each foil is 0.1 mm with a density of 1343 kg/m^3 [7]. The thickness of the outer two fibrous insulation spacer is 1.75 mm while the thickness of the interior each spacers are 4 mm. The density and thermal conductivity of fibrous insulation spacers are 220 kg/m^3 and 0.03 W/(m K) [8], respectively. The properties of materials and dimension of each layer are summarized in Table 1.The combined radiation/conduction heat transfer model is built based on finite element method using the commercial software package ANSYS 14.5. To reduce the complexity, the problem is simplified into a two-dimensional problem, and the JCG solver issued to solve the problem.

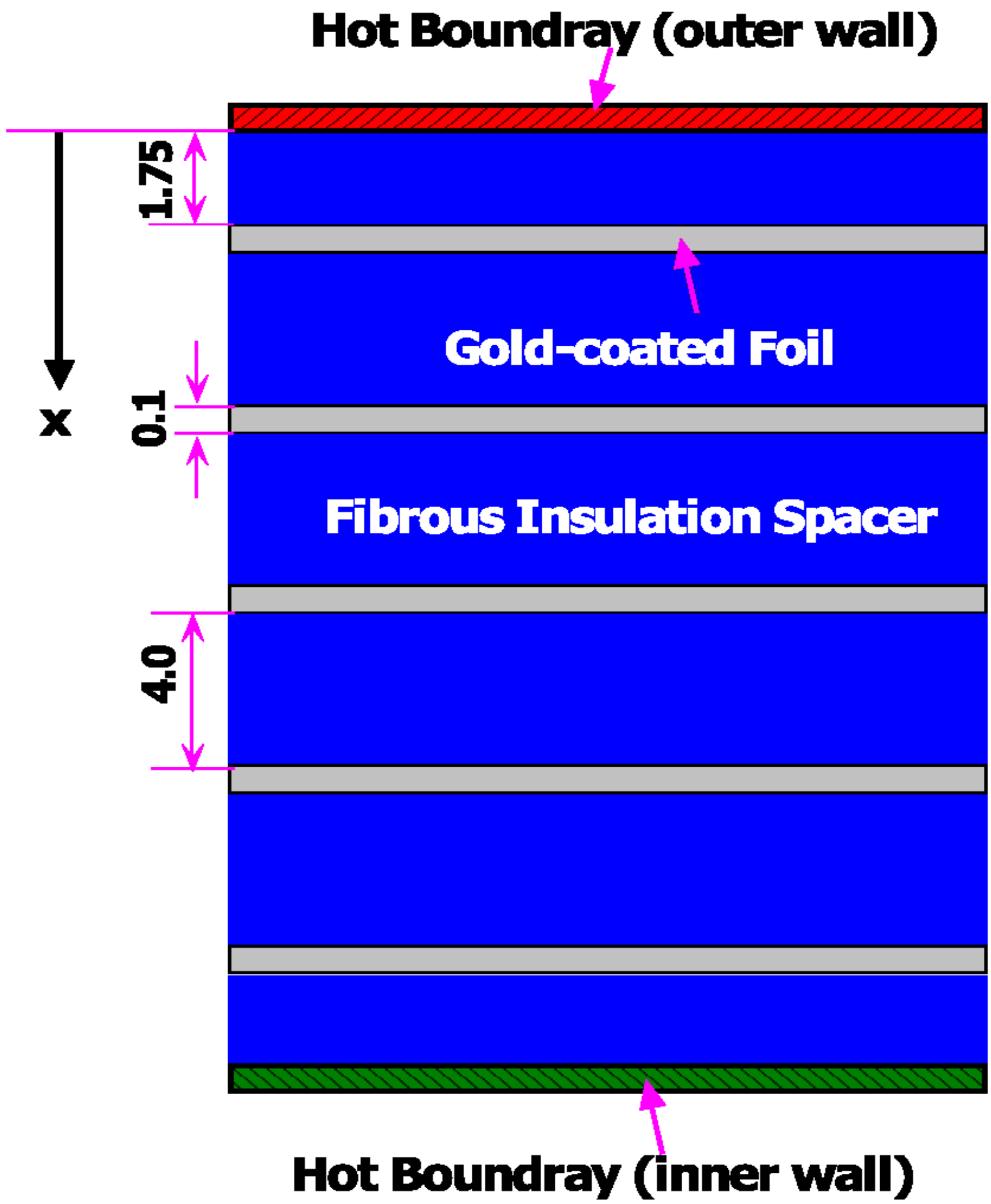

Fig3.1.Schematic of a typical multilayer insulation sample. The number of insulation spacers (N) is one more than the number of foils (N -1). The dimension is given in millimetre (mm).

Table 3.1 MATERIAL PROPERTIES AND DIMENSION OF EACH LAYER

Layers	Density (Kg/m3)	Thermal conductivity (w/mk)	emissivity	Thickness(mm)
Exterior insulation spacer	220	.03	_	1.73
Interior insulation spacer	220	.03	_	4
Foil	1343	100	0.02	0.1

3.1 ASSUMPTIONS

In this study solid heat conduction as well as thermal radiation is considered whilst convective heat transfer and gas conduction are ignored. The reason that natural convection is ignored is that the effect could be negligible compared to that of radiation heat transfer in such high-temperature situation. In addition, the insulation materials are assumed to be solid without porous under this circumstance, thus gas conduction is also ignored. Accordingly, the combined radiation/conduction heat transfer in high-temperature multilayer insulation is investigated in the present study.

3.2 HEAT TRANSFER MECHANISM

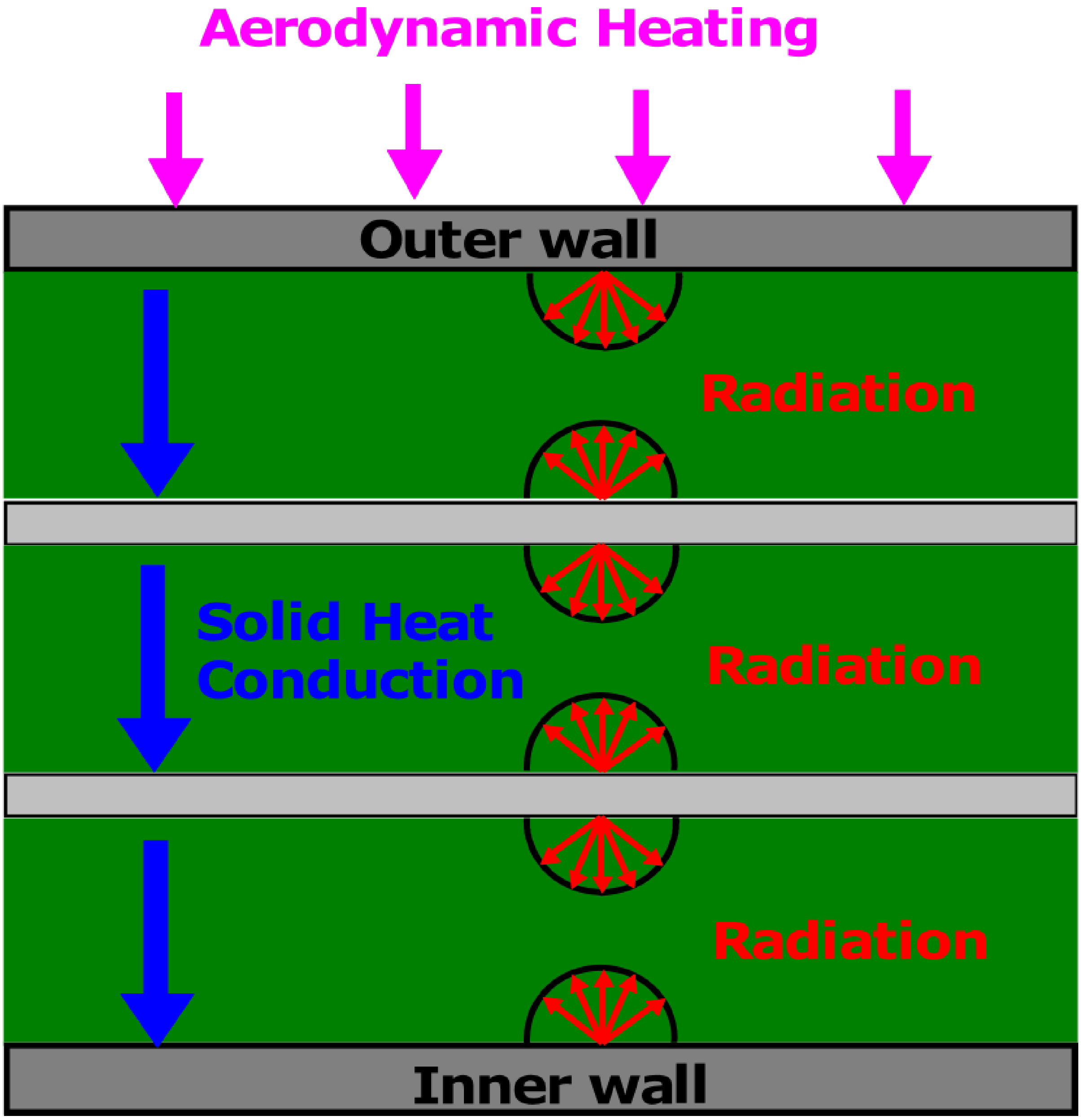

Fig3.2: represent Principles of the combined heat transfer model

The multilayer insulation is composed of fibrous insulation spacers, which is separated by thin ceramic/composite foils with gold coatings of high reflectance. Fibrous insulation spacer with a low thermal conductivity is confined between two opaque boundaries where one or more layers of thin foils/screens are paralleled. The fibrous insulation spacers and foils form a multilayer thermal protection system. Thermal radiation is absorbed, emitted and scattered by the insulation spacer material. Foils are made of opaque materials, which mean any kind of radiation cannot easily get through it, including light and thermal radiation. Although the foils/screens are very thin, they can emit and reflect radiation diffusely because of their opaque property.

During aerodynamic heating conditions, the heat transfer mechanism mainly involves conduction and radiation effects dominantly. The heat is conducted by the insulation spacers while the rest is radiated by the thin foils. Thus, to keep the bottom temperature within acceptable limits, the radiation heat transfer must be made large compared to the conduction heat transfer.

CHAPTER 4

METHODOLOGY FOR NUMERICAL ANALYSIS

In this current study a two dimensional finite element model of the multilayer insulation of width 20 mm is used for the study. The reason for selecting such geometry is because it is similar to that of one used by Karman Daryabeigi .The numerical analysis are done for different spacer materials that can be used .The effectiveness of both the materials can be understood from the analysis. Fibrous and micro porous spacer materials are analysed for the transient load according to Kamran Dariyabeigi. The temperature load is applied on the top surface or the boundary subjected to the aerodynamic heating conditions.

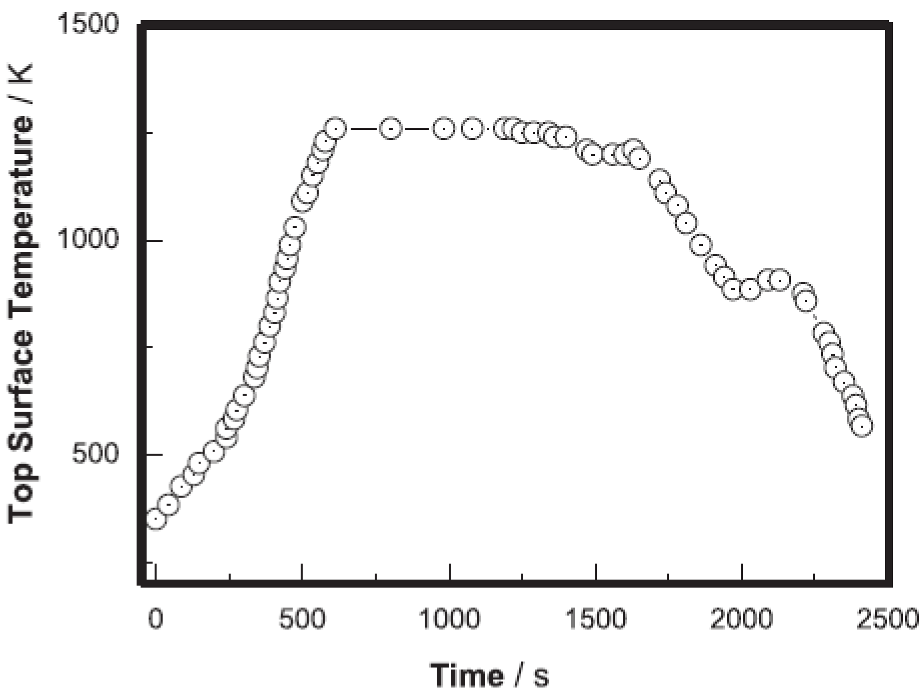

Fig4.1: Transient load applied on the surface

So the thermal load applied is the transient temperature corresponding to the time. The experimental load applied is the same and it is carried out for 2400s.The solver used for carrying out the numerical study is ANSYS Mechanical APDL.

For carrying out the experiment an element type need to be selected and for the current study the element type selected is 8 node 77 as plane 77 supports both radiation and conduction. For both the reflective foil and spacer materials the same element type is used .Initially a grid independence study conducted to determine the optimum mesh density for carrying out the analysis. The temperature load applied on the top surface is applied as a table. After numerous trial and error meshing three mesh sizes were selected to find the optimum among those .The geometry drawn in Ansys is shown below.

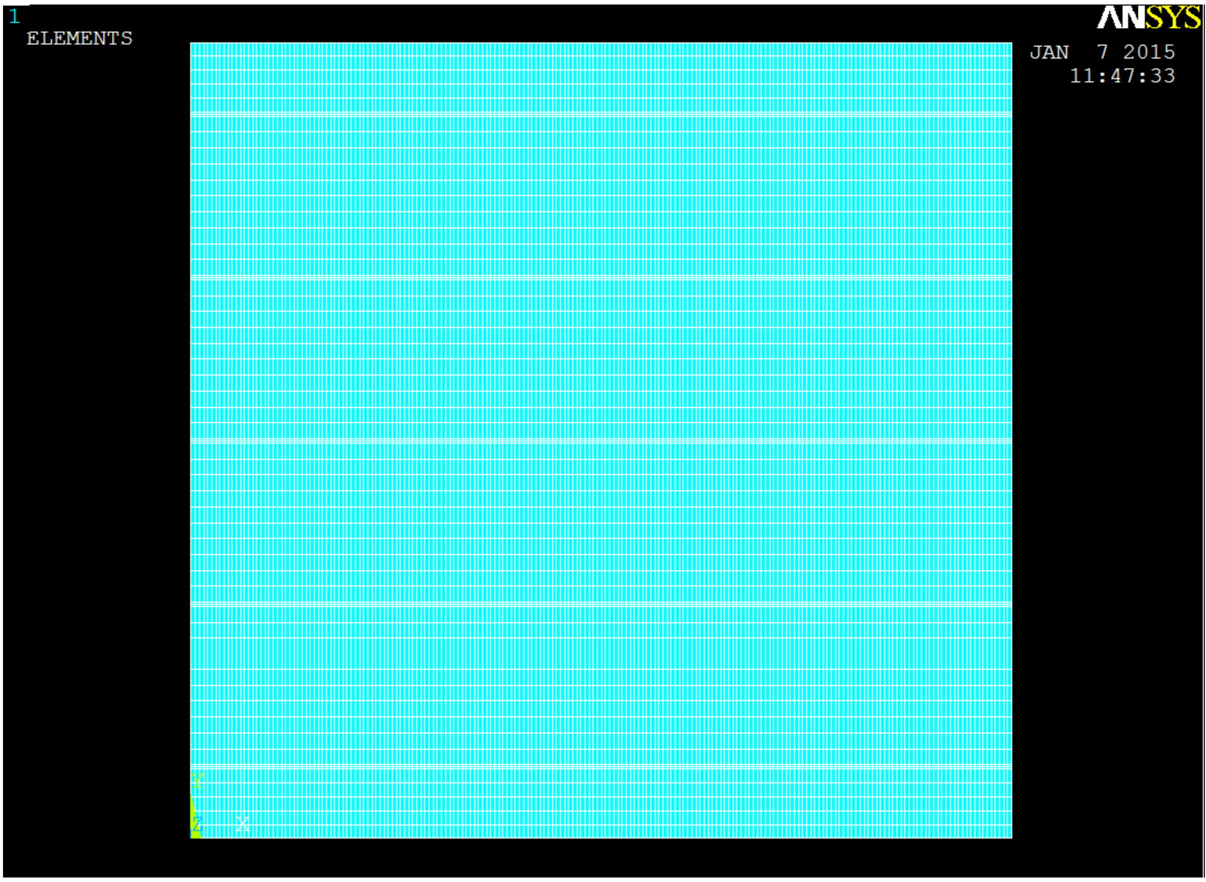

Fig 4.2: Ansys model of the MLI

Once the geometry is completed the above told three mesh density was used for meshing. A mesh density 30*100, 60*200 and 120*400 were selected. The analysis option is changed to transient as the default one is steady state analysis. Initial condition of 293 K is applied throughout the geometry. In the solution controls it is important to specify the time of the analysis which is 2400s in my study. Radiation is applied on the reflective foils and it is solved by using Radiosity Solver method. This method is offered in the ANSYS multi physics, ANSYS Mechanical, and ANSYS Professional programs only, the radiosity solver method also works for generalised radiation problems involving two or more surfaces receiving and emitting radiation. The method is supported by all 2-D and 3-D elements having a temperature degree of freedom. Radiation is the transfer of energy via electromagnetic waves. The waves travel at the speed of light, and energy transfer requires new medium. Thermal radiation is just a small band on the electromagnetic spectrum. Because the heat flow that the radiation causes varies with the fourth power of body's absolute temperature, radiation analysis are highly nonlinear .Initially the surfaces that are taking part in radiation are identified and radiation emissivity applied. On solution options it is important to give the value of Stefan Boltzmann constant. The default value needs to be changed. After setting its value the view factor is calculated for the geometry and it is computed. The radiation is applied on lines of the reflective foils and its emissivity applied is 0.02.

4.1 GOVERNING EQUATIONS AND BOUNDARY CONDITIONS

The governing equations in this study is the conservation of energy for each layer the conservation of energy equation is given by:

$$\rho c \frac{\partial T}{\partial t} = \frac{\partial}{\partial x}\left(k \frac{\partial T}{\partial x}\right) - \frac{\partial q_r''}{\partial x}$$

qr’’is the radiation heat flux density and x is the coordinate in the insulation thickness direction. C is the specific heat (J/kgK). The initial and boundary conditions are:

$$T(x,0) = T_0 = 293\text{ K}$$

$$T(0,t) = T_1(t)$$

$$T(L,t) = T_2(t)$$

Where T0 is the initial temperature of the whole multilayer insulation structure,T1 is the temperature load applied on the top surface of the insulation,T2 is the temperature of the bottom surface and L is the thickness of the whole sample .T2 should be within an acceptable limit. Since the surface of foil is opaque, it is considered as a diffuse reflection surface. It needs to satisfy the following condition of heat flux and temperature

$$T|_{x=x_s-0} = T|_{x=x_s+0}$$

$$-k_{\mathrm{m}}\frac{\partial T}{\partial x}\bigg|_{x=x_s} = -k_{\mathrm{eq}}^{s}\frac{\partial T}{\partial x}\bigg|_{x=x_s} + q_{\mathrm{r}}''$$

Where x(s) is the coordinate of the contact surface, km is the thermal conductivity of foil and k(eq) is the thermal conductivity of insulation material. The radiant flux qr’’ is given by:

$$q_{\mathrm{r}}'' = \epsilon\sigma\left(T_{\mathrm{h}}^4 - T_{\mathrm{l}}^4\right)$$

Where ϵ is the emissivity, σ is the Stefan-Boltzmann constant, T_h is the temperature in the hot side and T1 is the temperature on the cold side.

Table 4.1 INITIAL TEMPERATURE LOADS APPLIED ON TOP SURFACE

TIME (s)	TEMPERATURE (K)
0	293
125	400
250	600
375	740
500	1125
625	1250
750	1240
875	1235
1000	1230
1125	1225
1250	1210
1375	1200
1500	1170
1625	1170
1750	1160
1875	1100
2000	850
2125	875
2250	775
2375	600
2400	560

Table 4.1: Temperature vs Time

CHAPTER 5

GRID INDEPENDENCE STUDY

In order to find the optimum mesh density a grid independence study is done. As our aim is to make the surface of aircraft or space shuttles within the acceptable limits the temperature in the bottom surface of multilayer insulation is selected as criterion. Three mesh densities when subjected to the same transient load are studied and the error or deviation is calculated.

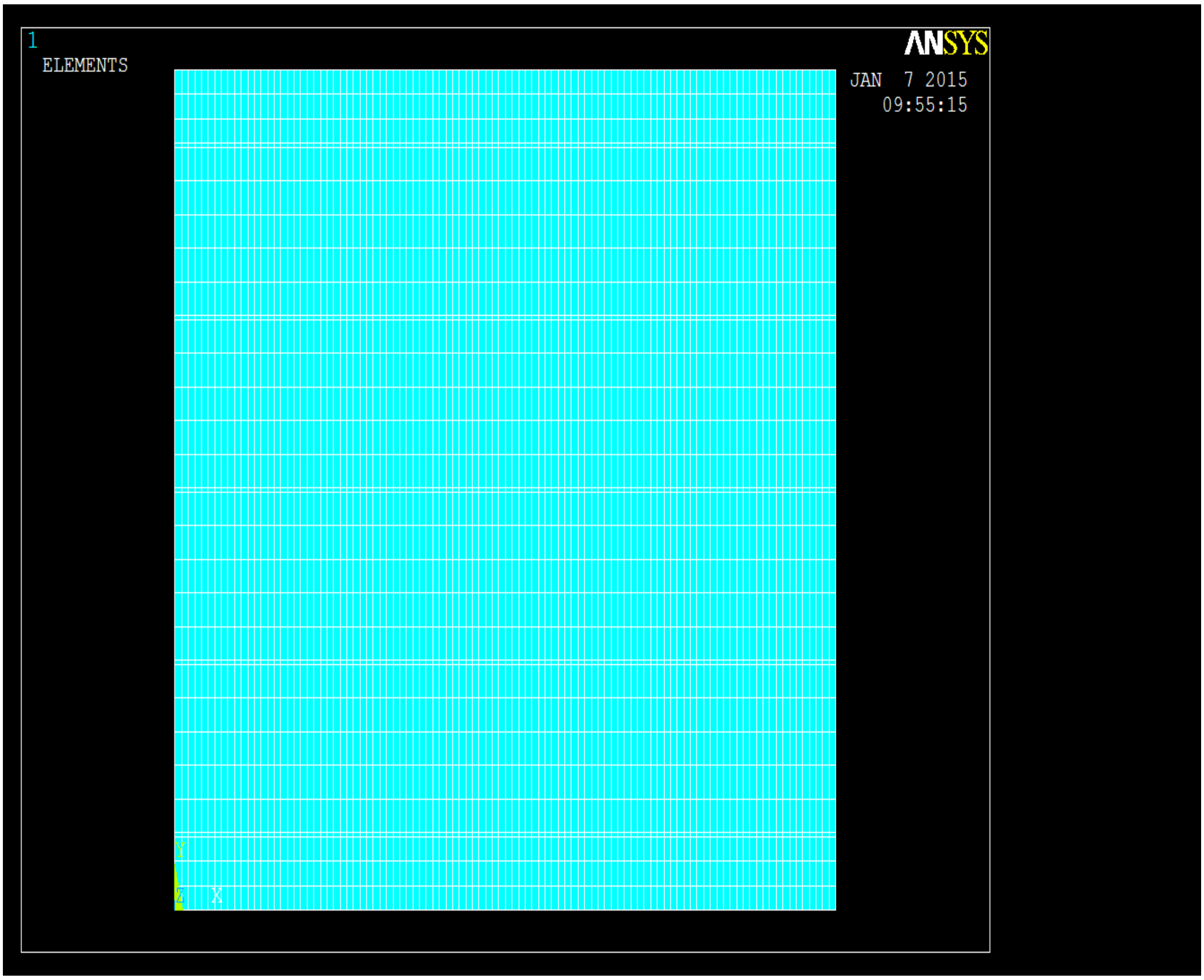

Fig 5.1: Mesh density 30*100

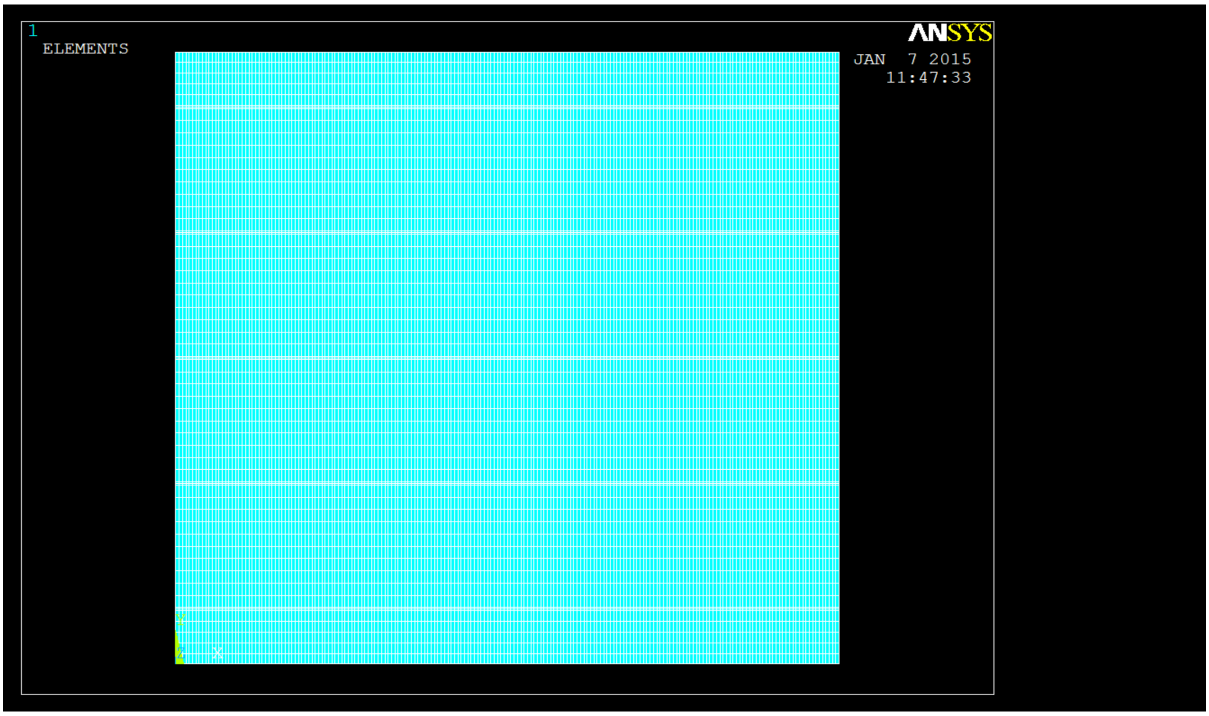

Fig 5.2: Mesh density 60*200

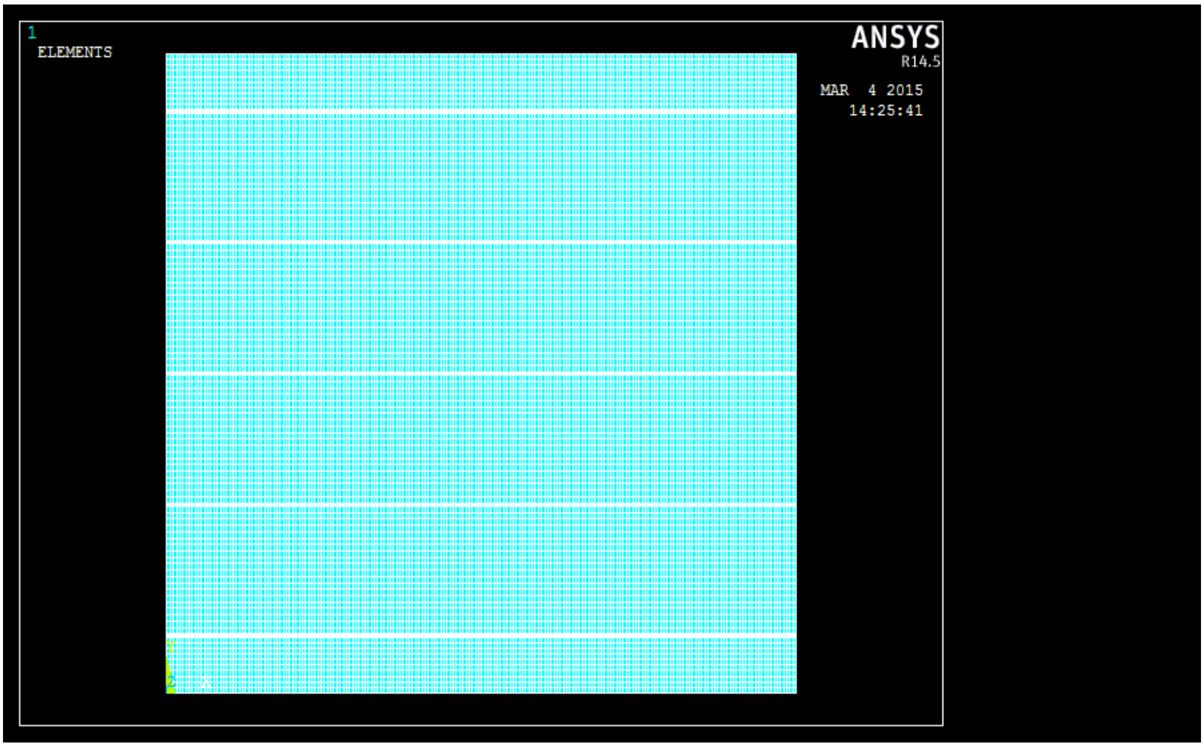

Fig 5.3: Mesh density 120*400

On carrying out the analysis on three different mesh densities the following observations were obtained on the low temperature surface. the temperature obtained for different time is tabulated and the deviation is calculated.

TIME (S)	T 30*100(K)	T 60*200(K)	T 120*400 (K)	X	Y
0	**293.129**	**293.04**	**293.042**	**.03**	**$6.82 * 10^{-4}$**
125	**293.626**	**293.40**	**293.403**	**.074**	**$1.02 * 10^{-3}$**
250	**297.23**	**296.82**	**296.822**	**.13**	**$6.73 * 10^{-4}$**
375	**308.162**	**307.58**	**307.589**	**.186**	**$2.92 * 10^{-3}$**
500	**328.549**	**327.85**	**327.852**	**.21**	**$6.1 * 10^{-4}$**
625	**360.377**	**359.53**	**359.592**	**.218**	**.017**
750	**400.012**	**399.19**	**399.203**	**.202**	**$3.256 * 10^{-3}$**
875	**439.456**	**438.65**	**438.663**	**.18**	**$2.96 * 10^{-3}$**
1000	**473.074**	**472.30**	**472.321**	**.16**	**$4.46 * 10^{-3}$**
1125	**499.624**	**498.91**	**498.936**	**.137**	**$5.21 * 10^{-3}$**
1250	**519.065**	**518.41**	**518.436**	**.12**	**$5.01 * 10^{-3}$**
1375	**532.777**	**532.19**	**532.216**	**.105**	**$4.88 * 10^{-3}$**
1500	**542.667**	**542.14**	**542.166**	**.092**	**$4.8 * 10^{-3}$**
1625	**548.966**	**548.49**	**548.516**	**.082**	**$4.74 * 10^{-3}$**
1750	**553.005**	**552.57**	**552.606**	**.072**	**$6.51 * 10^{-3}$**
1875	**555.578**	**555.2**	**555.234**	**.061**	**$6.12 * 10^{-3}$**
2000	**556.226**	**555.9**	**555.937**	**.051**	**$6.65 * 10^{-3}$**
2125	**552.631**	**552.35**	**552.283**	**.045**	**$5.97 * 10^{-3}$**
2250	**546.152**	**545.920**	**545.946**	**.0377**	**$4.76 * 10^{-3}$**
2375	**537.727**	**537.53**	**537.560**	**.031**	**$5.58 * 10^{-3}$**
2400	**535.785**	**535.59**	**535.626**	**.029**	**$6.72 * 10^{-3}$**

Table 5.1 Temperature of bottom surface from grid independence study

$$X = \frac{|T_{30\times100} - T_{120\times400}|}{T_{120\times400}} \times 100\%$$

$$Y = \frac{|T_{60\times200} - T_{120\times400}|}{T_{120\times400}} \times 100\%$$

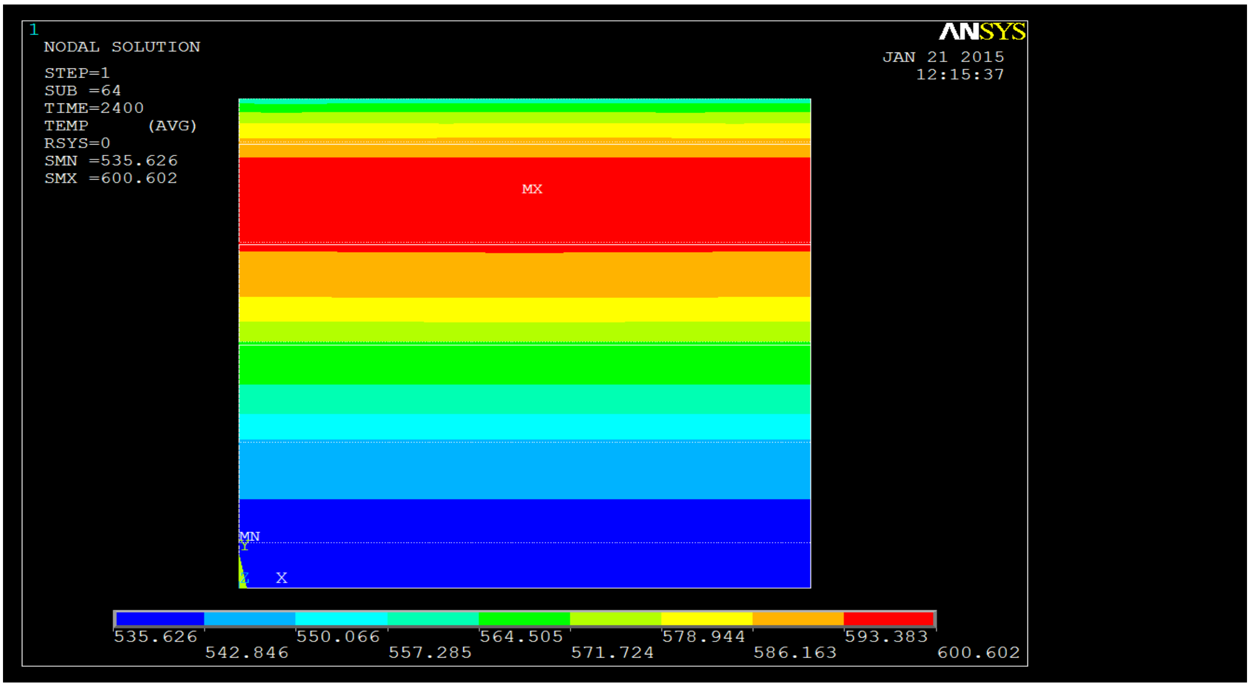

Fig5.4: Temperature distribution across insulation wall (200*60 mesh 50 time step)

Before simulating and analysing the heat transfer inside the multilayer insulation, a grid independence test was performed to investigate the influence of mesh density on the simulated results. Three mesh densities were tested: 30*100, 60*200 and 120*400.The temperatures of the bottom surface of the thermal insulation structure with different mesh density at some selected time are listed in Table 5.1. The temperature in the finest meshes is set as a criterion. The deviation is defined as the percentage of the absolute value of the difference of the temperature of other density compared to the criterion, which is also included in Table 5.1. It can be seen that the average deviation of the mesh density 30 *100 is 0.107%, while that of the mesh density 60*200 is 0.004%. The deviation of below0.1% is acceptable considering the numerical accuracy and computing time. Therefore, the mesh density of 60 _ 200 is adopted for later prediction. Figure represents the typical mesh containing quadrilateral elements, which ensure numerical accuracy

CHAPTER 6

ANALYSIS OF MLI

6.1 ANALYSIS OF MLI- SILICA AEROGEL AS THE INSULATION MATERIAL.

Micro porous materials are having a moderate density in the range of 100-250 Kg/m^3 and low thermal conductivity in the range of .02-04w/mK. Thus by theoretical base they are a better insulation material when compared to fibre materials. In the present study among the micro porous materials silica gel is used for the numerical study. Silica Aerogel having a density of 1 Kg/m^3 and thermal conductivity .003W/mK and is used here for the analysis. A specific heat capacity of 840 J/KgK is used here. The dimension of the MLI sample is the same as the basic structure. The bottom surface temperature for different time ranging from 0 – 2400 s is noted. The initial and boundary conditions are same as the above analysis.

6.2 EFFECT OF DENSITY OF THE SPACER MATERIAL

The effect of varying density on the performance of MLI sample is analysed for the same MLI sample using silica Aerogel as the insulation spacer materials. The dimension of the sample is 20 mm and the entire initial and boundary conditions are same as the above. Three densities are selected for the studies. The densities selected for studies are 220 $Kg/m^{3,}$ 140 Kg/m^3, 70 Kg/m^3. The density is proportional to the mass of the spacer material since volume is assumed to be fixed thus for a given heat transfer, to obtain a lower temperature, density must be high.

6.3 EFFECT OF EMISSIVITY ON THE BOTTOM SIDE TEMPERATURE

The emissivity of the reflective foils may also affect the heat transfer across the MLI sample. To determine the effect of emissivity on the bottom surface temperature three emissivity of foils are made used. The effect of increasing the emissivity on temperature distribution is analysed. The three different emissivity of foil material used for analysis are .02, 05 and .08. The spacer used here are alumina. So without changing the density and spacer material the impact of changing emissivity on the temperature distribution is studied.

CHAPTER 7
RESULTS AND DISCUSSIONS

7.1 EFFECT OF THE LAYOUT OF FOILS

There are three layouts/arrangements for the space between the interior reflective foils: uniform, increasing and decreasing as the foil approaches the cold boundary, as shown in Fig.7.1. It is noted that in the above sections the space between two interior foils was uniform. In this section, a multilayer insulation structure with the total thickness of 20 mm is investigated to observe the layout of the reflective foils. A typical case with five reflective foils (six layers) is designed here for the multilayer insulation structure with a thickness of 20 mm. In Fig. 7.1(a), the space between two foils is the same with the thickness of 3.25 mm.

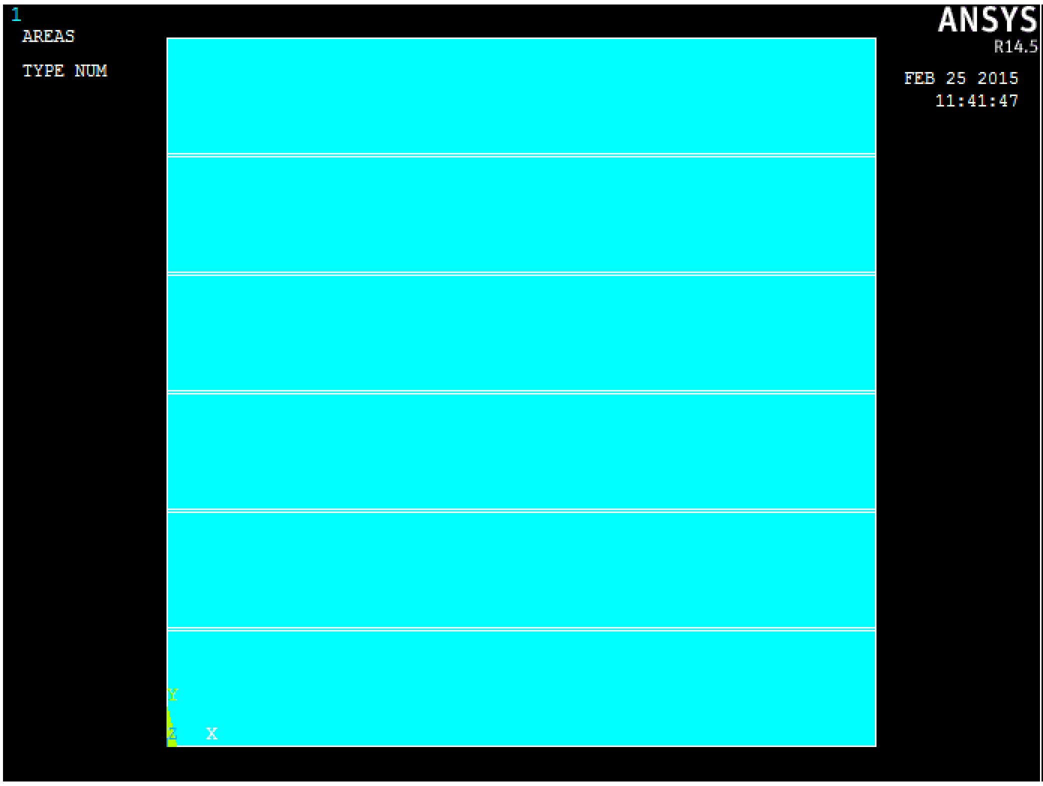

Fig 7.1(a): Uniform Spacing of the foils

In Fig. 7.1(b), the space is increasing as the foil approaches the cold boundary, and the space between the first and second foils is 1mm, and the space between the last two foils is 5.5 mm. The space increases in an arithmetic sequence. In Fig. 7.1(c), the space between foils is decreasing as the foil approaches the cold boundary. The space between the first and second foils is 5.5 mm, and the space between the last two foils is 1 mm. The space decreases in an arithmetic sequence.

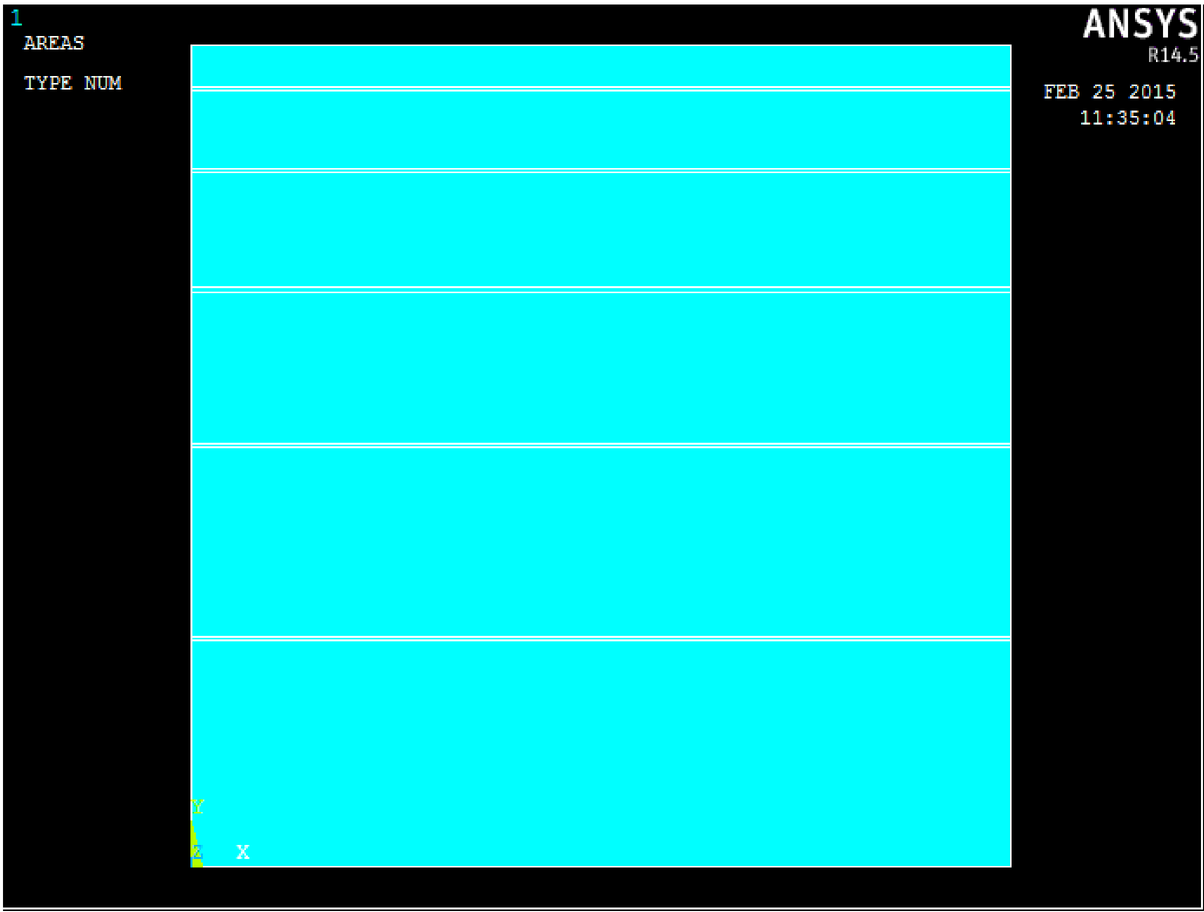

Fig 7.1 (b): Increasing spacing of the foils

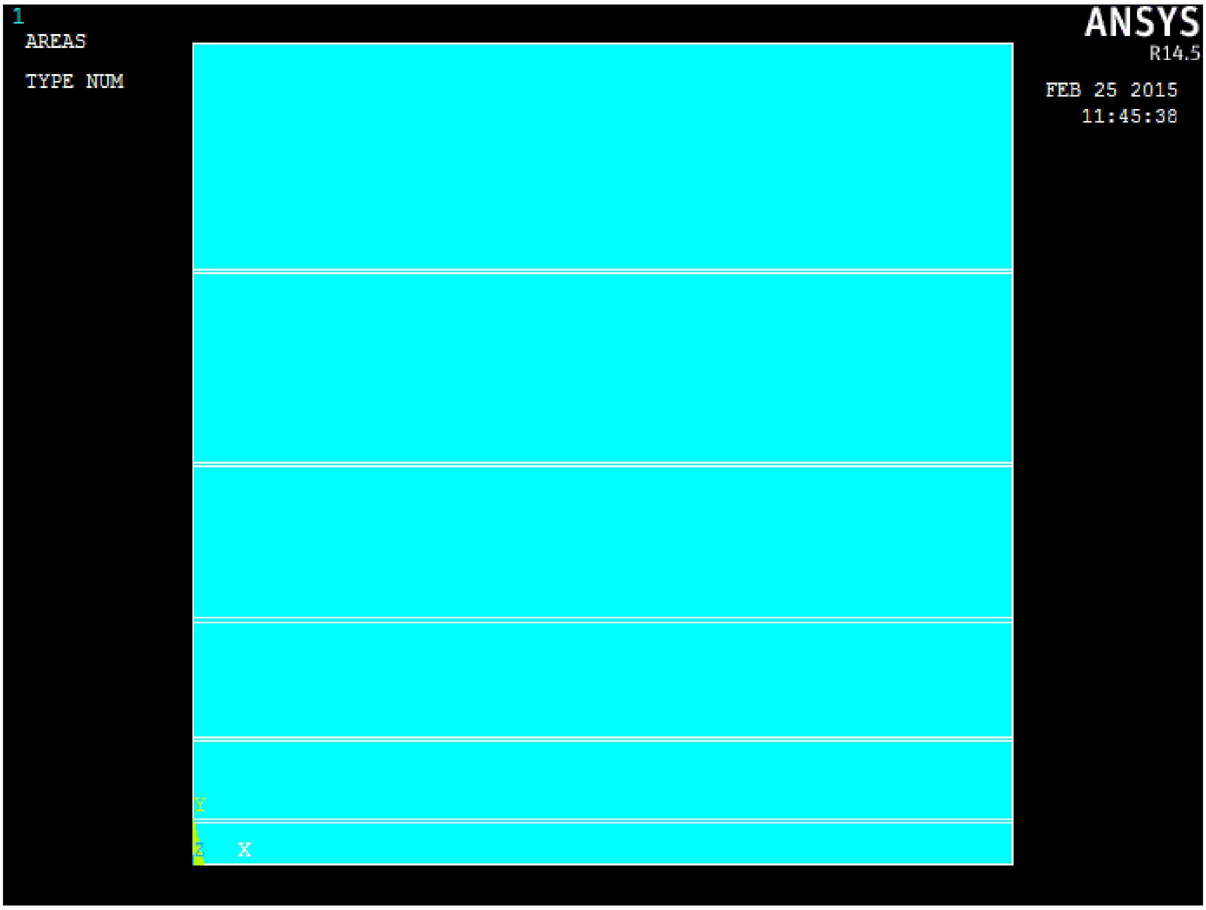

Fig 7.1(c): Decreasing spacing of the foils

The effect of the layout of the foils on the temperature of the bottom surface is shown in Fig. 7.2. It can be seen that, the temperature trend of the different layouts is almost the same before1000 s. However, after this time, the layout with the increasing space has slightly higher temperature, and the layout with the decreasing space has the lowest temperature. Overall, the difference is quite small, indicating the layout of foils has little effect on the thermal insulation performance through the multilayer insulation structure under this condition. This might be because that at first the temperature is not very high and the heat has not been accumulated, the impact of radiation heat transfer is not significant. This means the radiation effect is almost the same for different cases. However, after the time of 1000 s a large amount of heat has been stored in the spacers since the spacer material has a large thermal capacity, and thus the temperature of the whole insulation layers is getting higher. The space between foils near the bottom surface is larger than that of other conditions, therefore, the radiation between them is not as strong as other conditions, and then more heat is conducted to the bottom surface which leads to bottom surface temperature being high.

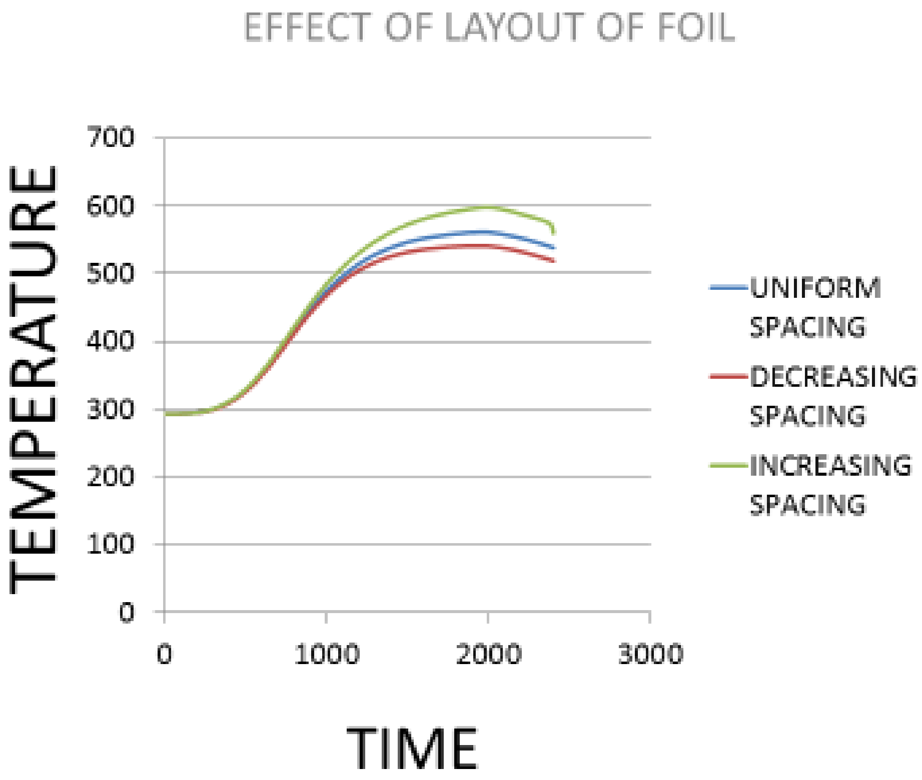

Figure: 7.2 Eeffect of foil layout

The temperature distribution across the boundary wall for different arrangement of foils that is increasing, decreasing and uniform arrangement is given in figure 7.3.The bottom temperature of increasing, decreasing and uniform spacing are 584.101k, 518.93k, 538.25k respectively.

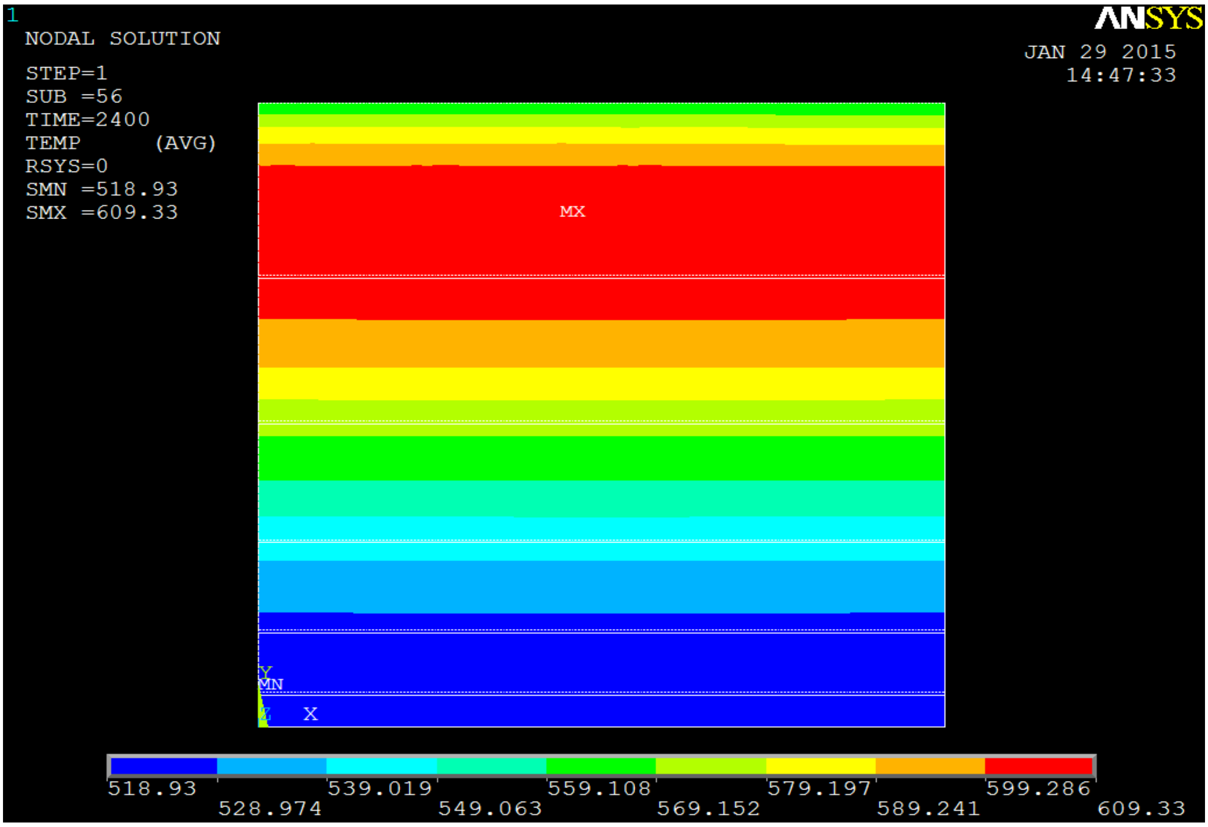

Figure 7.3.a: Temperature distribution of decreasing foil spacing

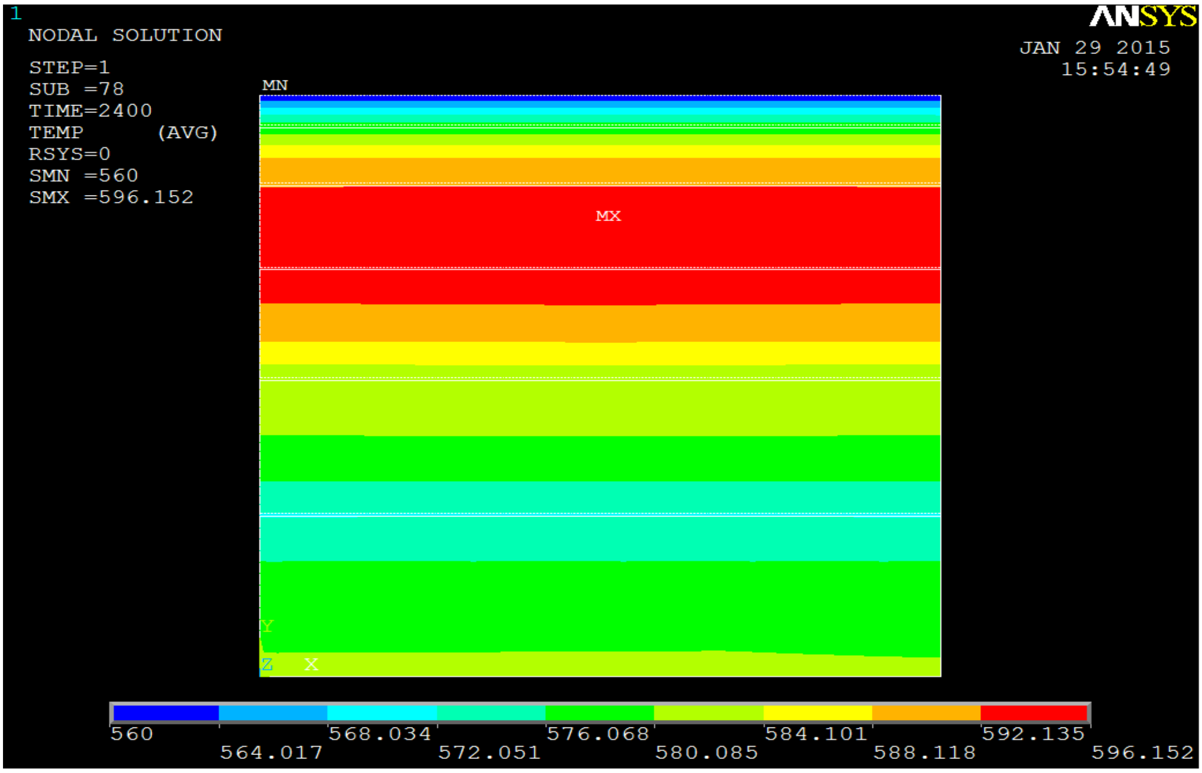

Figure7.3.b: Temperature distribution of increasing foil spacing

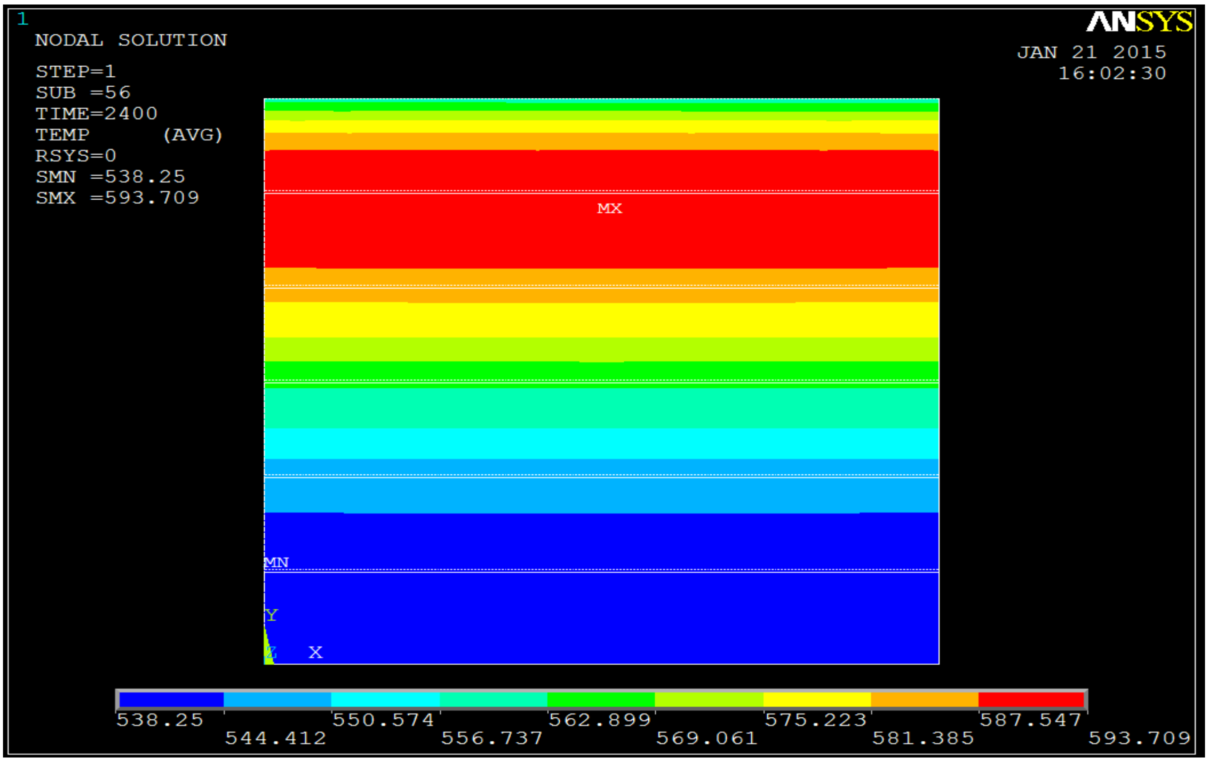

Figure 7.3.c: Temperature distribution of uniformly spaced foils

7.2 EFFECT OF DENSITY OF FIBER MATERIAL

As is concluded above, when the number of insulation layers is 6, the thermal insulation has the best performance. Therefore, to investigate the effect of the density of the fibre (insulation) material, a structure with 6 layers of insulation is chosen for study. The boundary condition is the same as mentioned above. The bottom surface temperature under different densities of insulation material is shown in fig 7.5It is obvious that as the density of the insulation material increases, the bottom temperature decreases. To comprehend the result better, the below equations are considered:

$Q=cm\Delta t$

Where $m=\rho V$

Where Q stands for the heat absorbed by the insulation material, m stands for the mass of insulation material, Δt stands for the increase of the temperature of the insulation material, ρ stands for the density of insulation material, and V stands for the volume of the insulation material. The volume is assumed to be a constant (the total thickness is fixed), thus an increase of the material density lead to an increase of the mass. Then if the special heat is a constant, to increase the same value of temperature, more heat is absorbed. This indicates more heat is stored in the insulation material, thus the temperature of the bottom surface is lower

The temperature distribution across the wall at different densities are given below. The densities of materials are material 1-220kg/m3, material 2-140kg/m3, material 3-70kg/m3.The bottom surface temperatures at 220kg/m3,140kg/m3, 70kg/m3 densities are 535.626K, 524.226K, 507.004K.

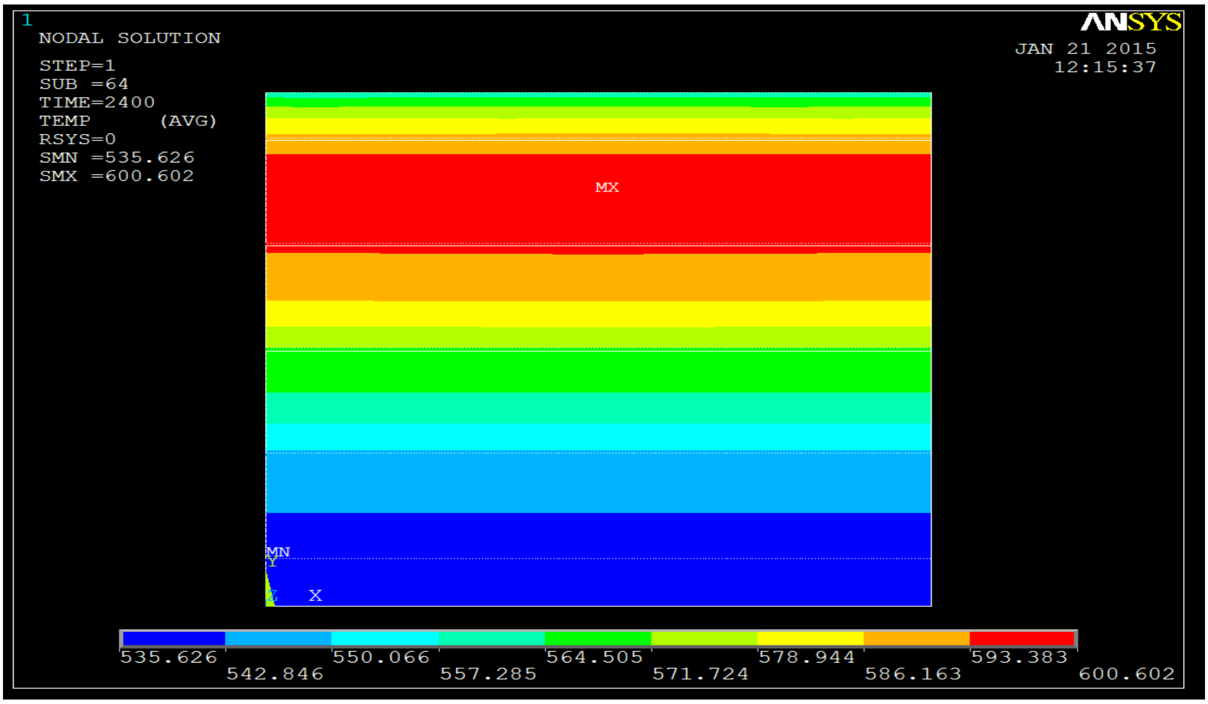

Figure 7.4.a: Material 1-density: 220 Kg/m^3

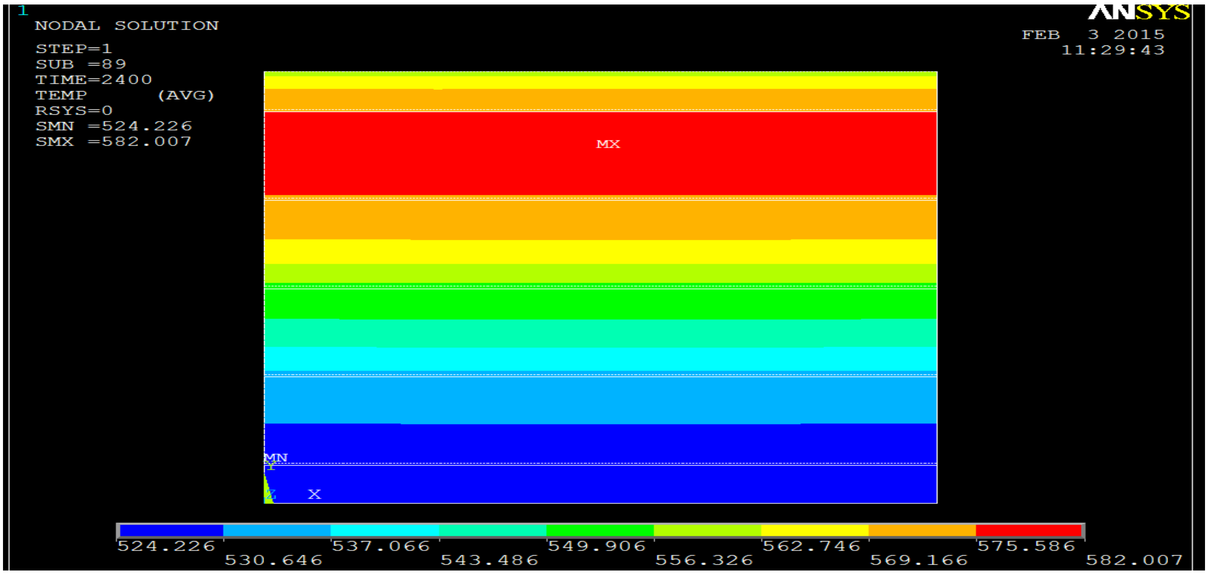

Fig.7.4 b: Material 2- Density: 140Kg/m^3

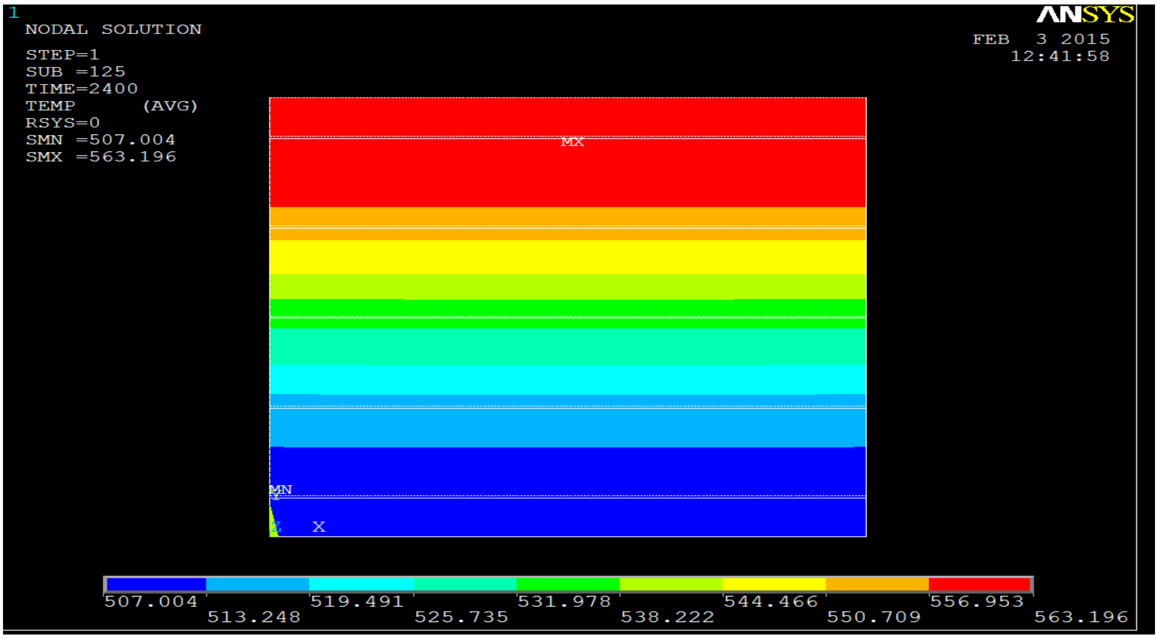

Fig.7.4.c: Material 3-density: 70 Kg/m^3

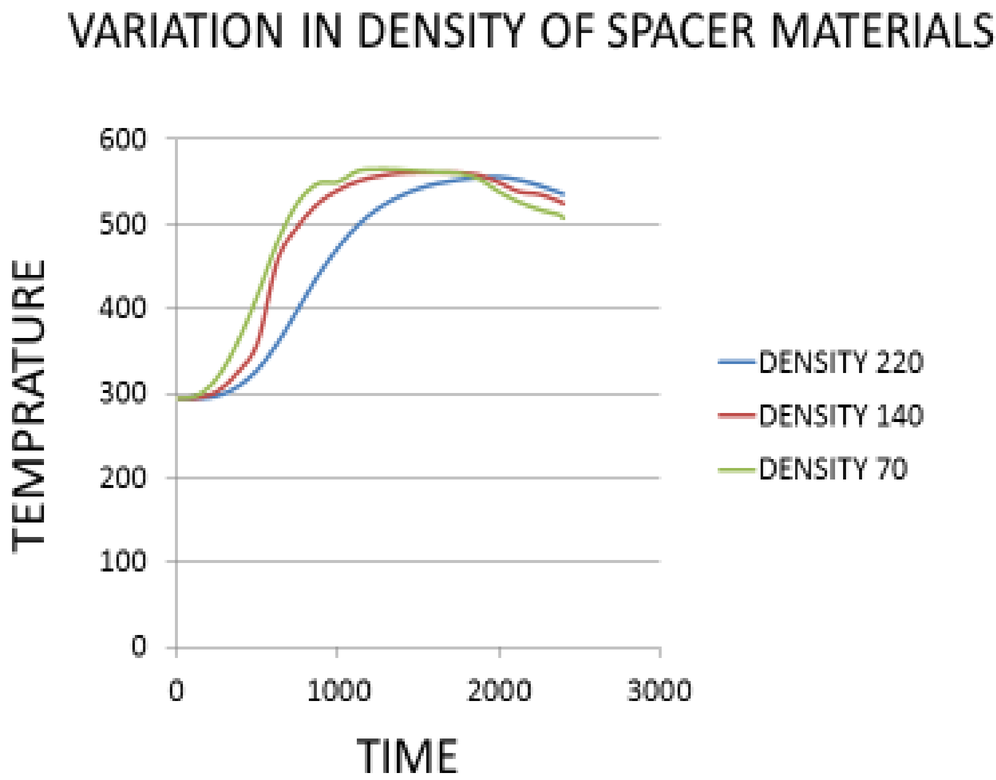

Temperature- Kelvin Time - seconds

Fig 7.5: Variation of density of spacer materials

7.3 EFFECT OF CONDUCTIVITY

As is concluded above, when the number of insulation layers is 6, the thermal insulation has the best performance. Therefore, to investigate the effect of the density of the fibre (insulation) material, structure with 6 layers of insulation is chosen for study. The boundary condition is the same as mentioned above. The bottom surface temperature under different conductivities of insulation materials is shown in Fig7.7. It is obvious that as the conductivity of the insulation material increases, the bottom temperature increases. To comprehend the result better, the below equations are considered:

$Q = -kA\ (dt/dx)$

where Q stands for the heat conducted by the insulation material, k stand for the conductivity of insulation material, A stands for the area, area and temperature gradient are constant then as the conductivity increases bottom surface temperature increases. The materials used as the spacer materials are alumina silica, composite of alumina and silica gel. Conductivities of alumina silica, composite of alumina and silica gel are .03w/m K, 28W/m K, and .003W/m K respectively. The temperature distribution across the insulation layer are given in figure.

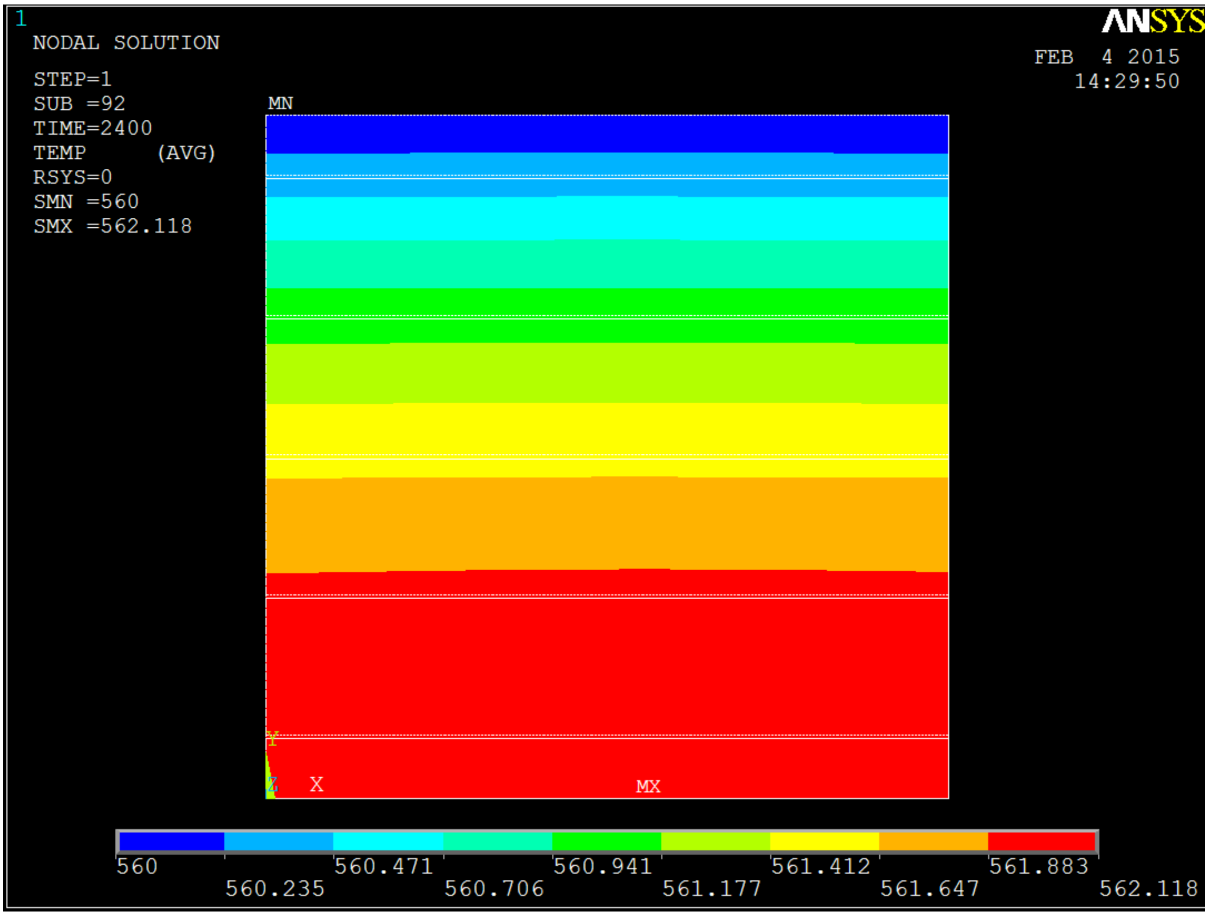

Fig7.6.a: Material 1: Conductivity=28 W/mK

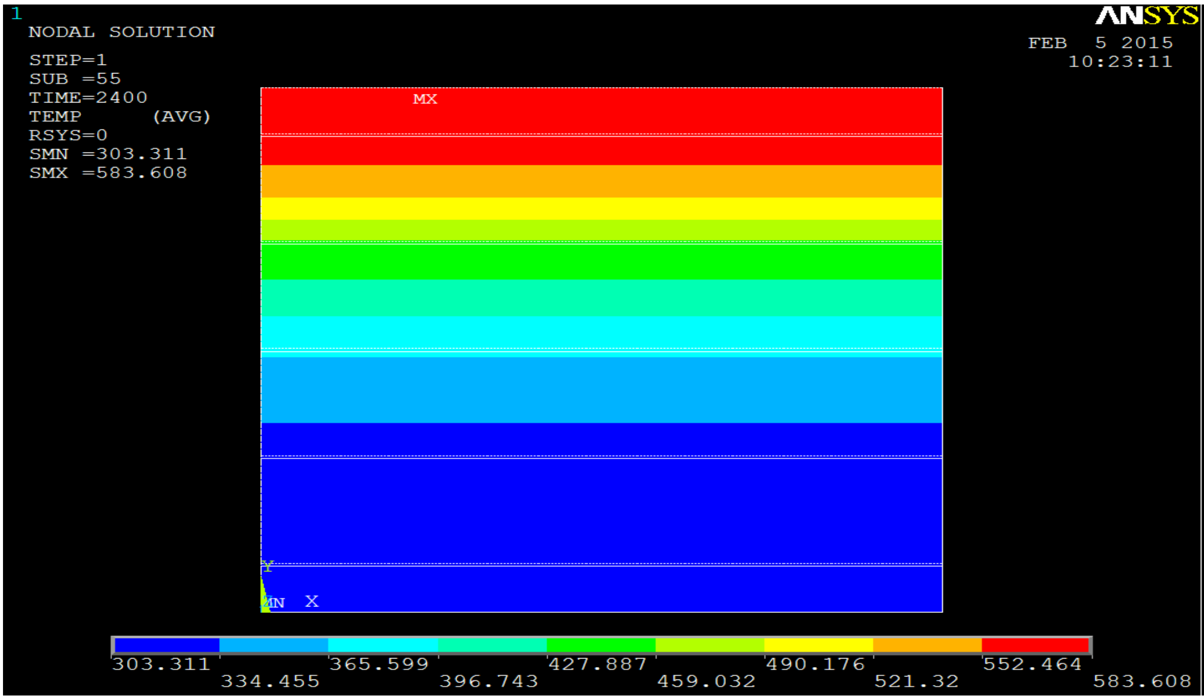

Fig:7.6 b: Material 2-Conductivity=0.003W/mK

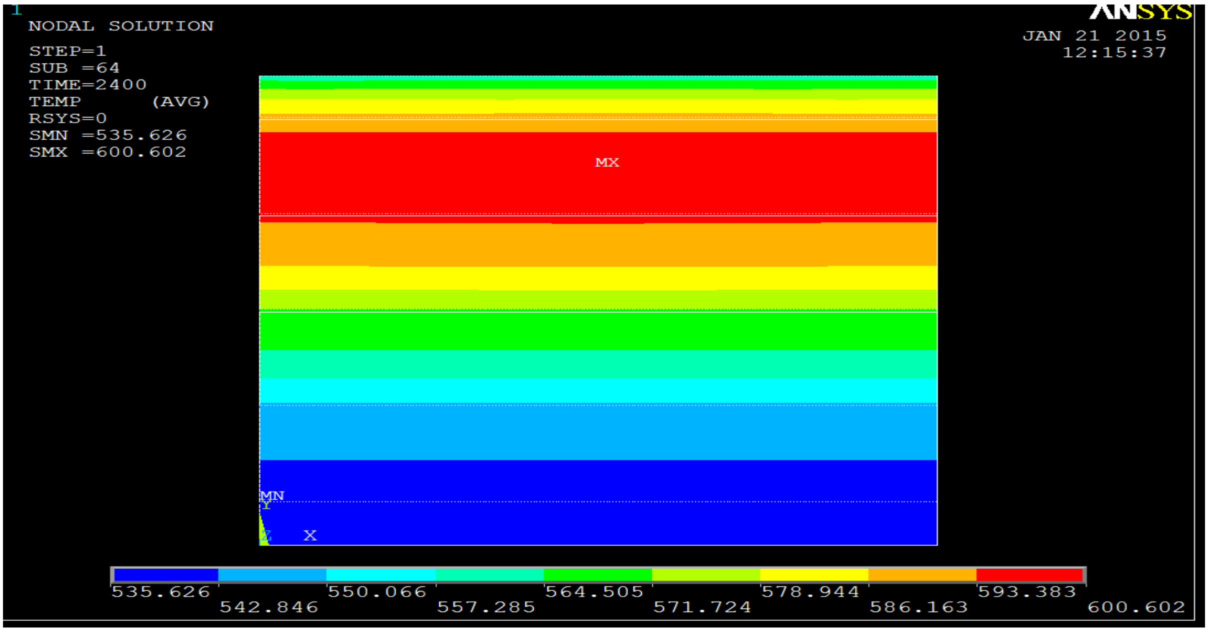

Fig 7.6.c: Material 3: Conductivity=100W/m K

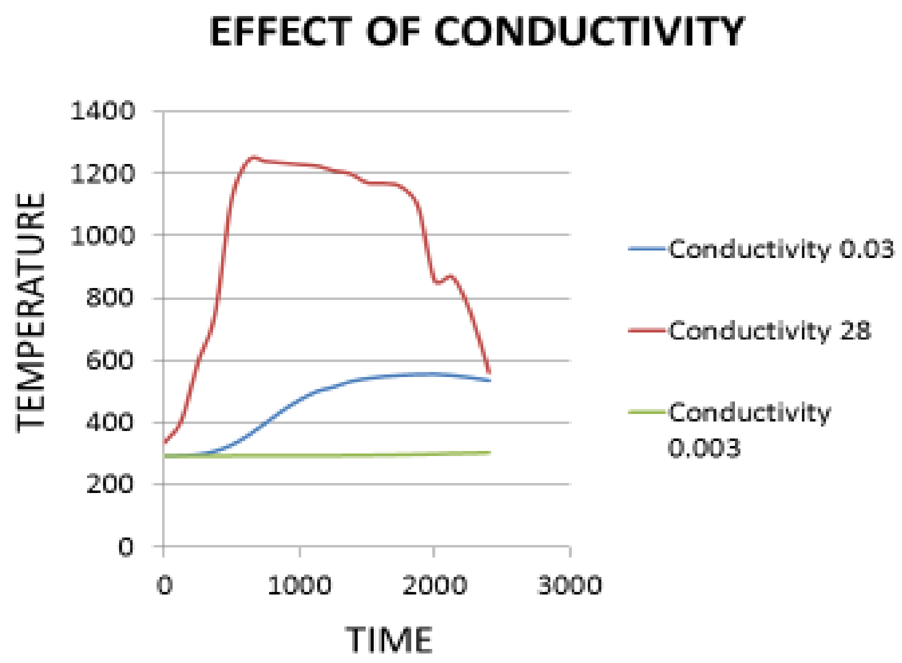

Temperature- Kelvin Time- seconds

Fig7.7: Effect of conductivity

7.4 EFFECT OF EMISSIVITY OF FOIL

When the emissivity of the foil is to be investigated, the number of insulation layers is also kept 6. The boundary condition is still the same as above. Fig. 7.9 presents a comparison of the bottom surface temperature under different emissivity of reflective foils. It is found that the bottom temperature decreases with the increase of the emissivity as observed in the figure. To explain the phenomenon better the equation given below is considered.

$$q_r'' = \epsilon\sigma\left(T_h^4 - T_l^4\right)$$

Where ε is the emissivity and σ is stefan-boltzmann constant, the heat flux caused by radiation heat transfer, q_r'' would be increased with increasing of the foil emissivity.

This means the effect of the radiation is becoming greater as the emissivity increases. Therefore under this circumstance, more heat is dissipated and is emitted to the environment through radiation heat transfer process inside the insulation material between the foils. As results, such case reduces the amount of heat conducted to the bottom, and thus lower temperature of bottom surface is achieved. The emissivity of materials are 0.05, 0.08 and .02 respectively and their temperature distribution across wall is given below

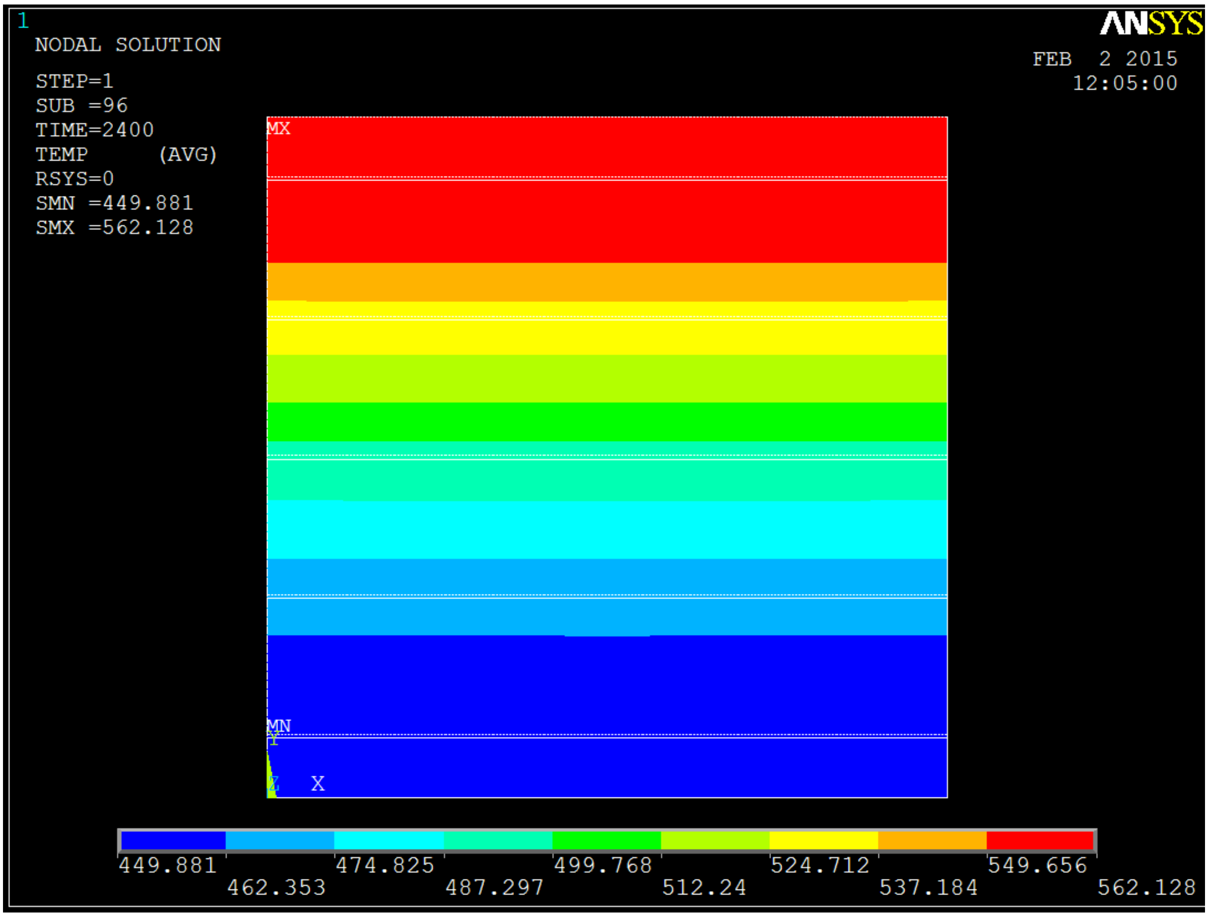

Fig 7.8.a: Material-1:Emissivity0.05

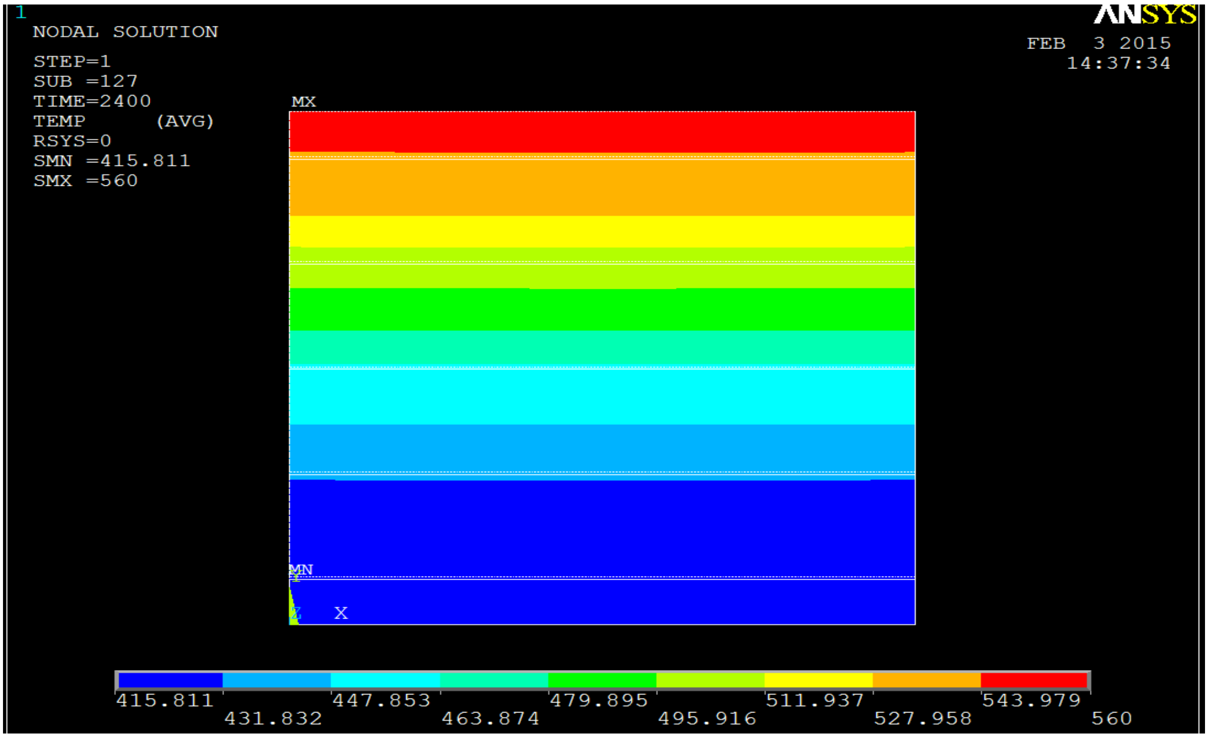

Fig7.8.b: material-2- Emissivity=0.08

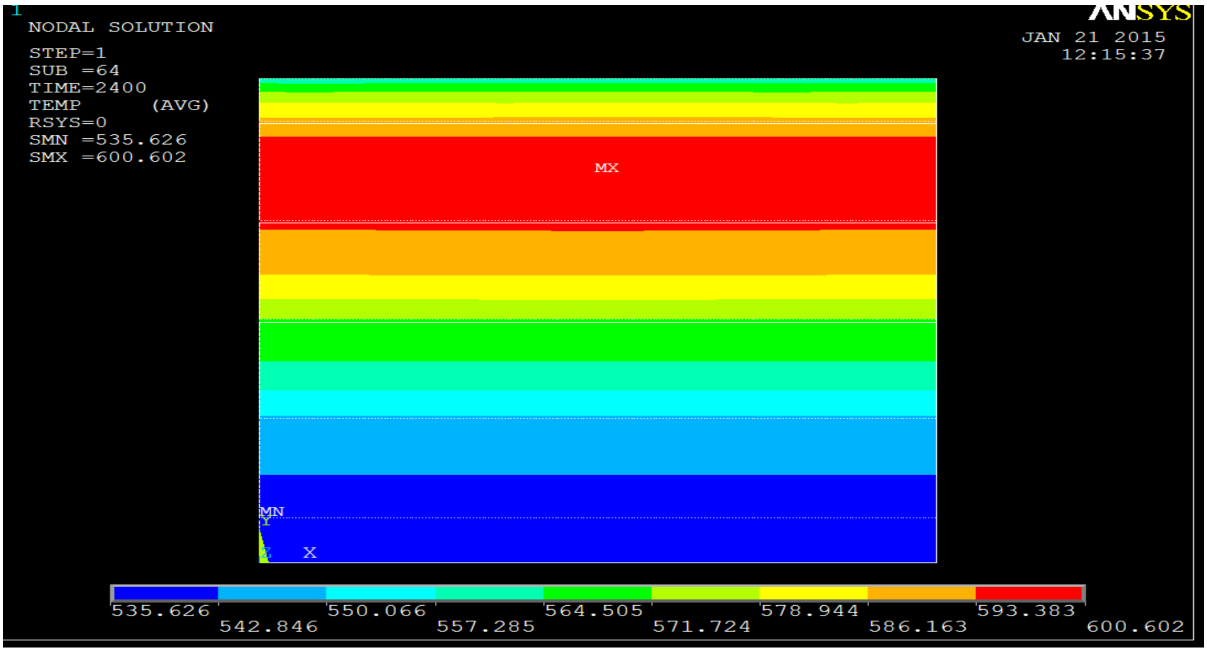

Fig 7.8.c: Material-3: Emissivity=0.02

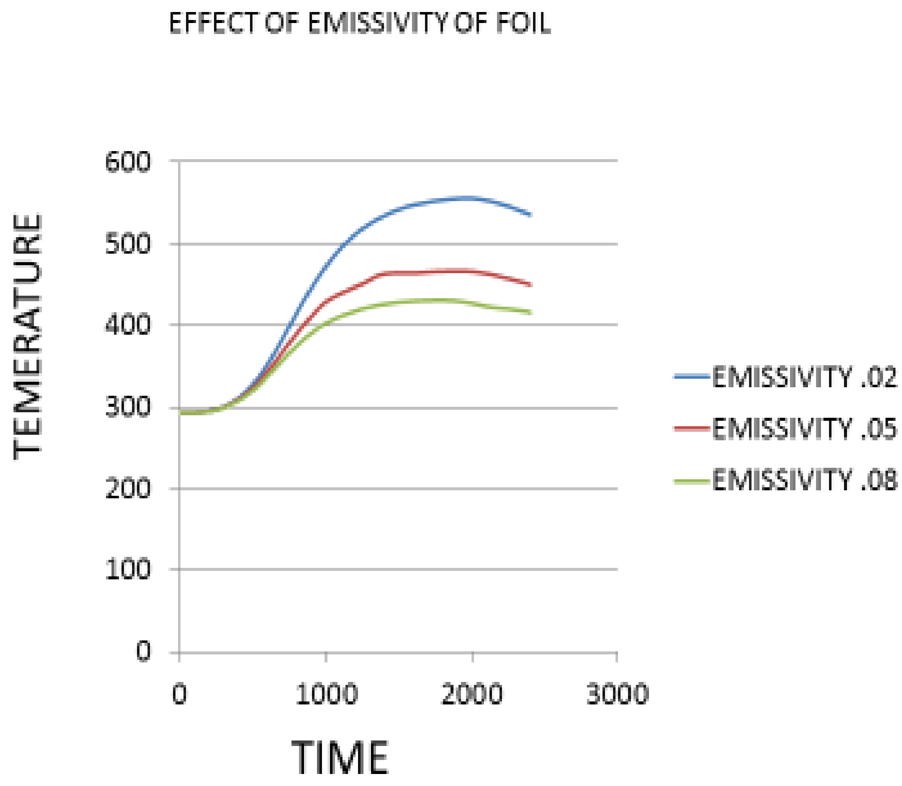

Temperature – Kelvin Time - seconds

Fig 7.9: Effect of emissivity of foil

7.5 ANALYSIS OF MLI USING SILICA AEROGEL

Instead of using a fibrous material using a micro porous material results in the heat transfer as shown in fig7.10.The temperature obtained in the bottom surface while using silica aero gel is 336.551 K. Thus we can infer that a micro porous material is a more effective insulation when compared to that of glass wool or fibrous insulation. The maximum temperature is not at the top surface where the transient load is applied whereas it is somewhat below the top surface. It is because of the fact that temperature is conducted to the bottom surface initially and because of the increase on density of the silica aero gel more amount of heat is conducted initially.

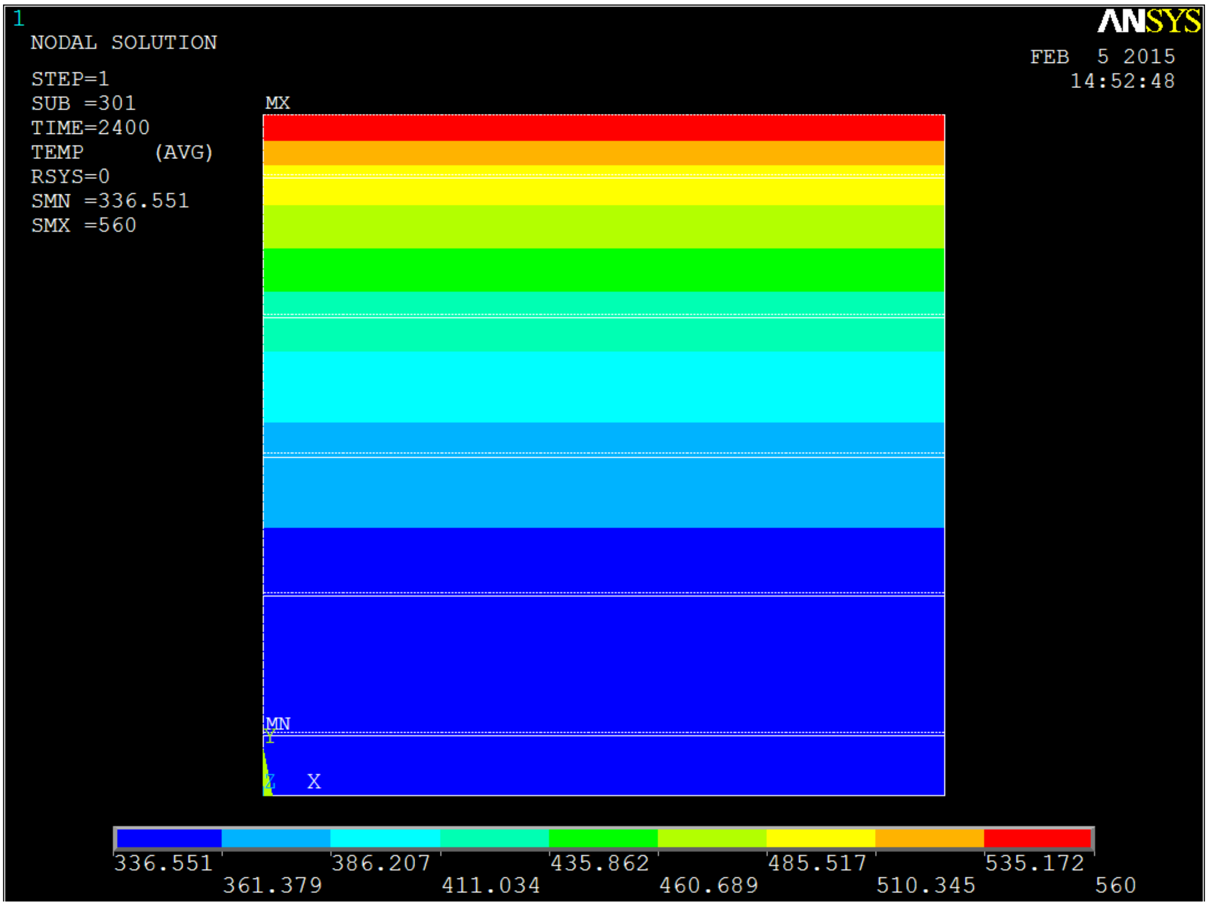

Fig.7.10: Spacer Material-Aerogel

Properties of Aerogel material is:

1. Thermal conductivity: 0.003W/m K

2. Density: 1Kg/m^3

3. Specific heat capacity: 840 J/Kg K

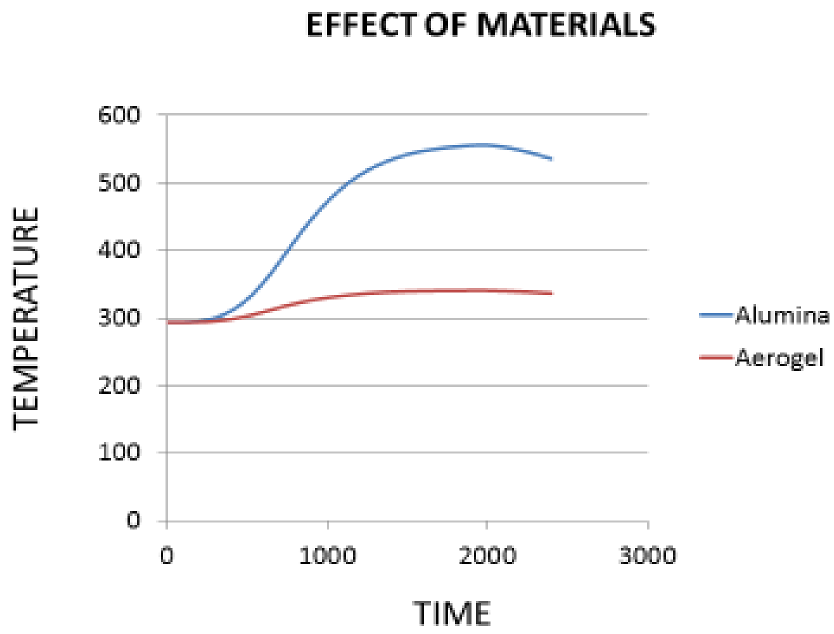

Temperature – Kelvin Time - seconds

Fig 7.11: Effect of different spacer materials

CHAPTER 8

CONCLUSIONS

In the present study a numerical analysis of multilayer insulation subjected to high temperature transient load is done. The numerical analysis is done to study the effect of aerodynamic re-entry conditions on multilayer samples. a two-dimensional numerical model was built to model the combined radiation and conduction heat transfer in high temperature multi-layer insulations. It is validated by a comparison with experimental data from a reference case. The temperature trend and the maximum temperature of the bottom surface are obtained under several simplifications, assumptions and a nonlinear thermal analysis and the obtained minimum temperature is about half of the maximum value. A summary of the major findings is presented as follows:

1: The layout of the foils does not have much effect on the thermal performance under the present model condition. The uniform layout is conservatively suggested.

2: It is obvious that as the density of the insulation material increased the bottom surface temperature decreases.

3: it is observed that the temperature of the bottom surface is lower when the emissivity of foils is higher.

4: it is found that when the conductivity of spacer material increases, the bottom surface temperature was also increases proportionally.

5: it was observed that silica aero gel prove to be the better of two insulation material being used in this study.

REFERENCE

[1] **Kamran Dariyabeigi**, Thermal Analysis and the Design of multilayer Insulation for re-entry aerodynamic heating, AIAA 2001-2834.

[2] **Daryabeigi, K**, Design of High temperature Multilayer Insulation, Ph. D. Dissertation , *University of Virginia*, May 2000.

[3] **Huang Can, Zhang Yue**, Calculation of high – temperature insulation parameters and heat transfer behaviours of multilayer insulations by inverse problem method, 27(4): 791-796(2014).

[4] **Peng Li, Huier Cheng**, Thermal analysis and the performance study for multilayer perforated insulation material used in space, Applied Thermal Engineering 26(2006) 2020-2026.

[5] **Ozisick, M.N**, Radiative Transfer and Interactions with Conduction and Convection, 1973, John Wiley &sons,Inc.

[6] **M. Spinnler, R. F Edgar, R. Viskanta**, Studies on high temperature multilayer thermal insulations, Int. J. Heat Transfer 47 (2004) 1305- 1312.

[7] **Shu-yuan Zhao, Bo – ming Zhang, Xiao- dong He,** Temperature and pressure dependent effective thermal conductivity of fibrous insulation, International Journal of Thermal Sciences 48(2009) 440-448.

[8] **Sparrow, E.M and Cess R.D,** Radiation Heat Transfer, Augmented Edition, 1978, Mc Graw-Hill Book Company.

[9] **M. Grujicic, C.L Zhao, S.B Biggers,** J.M. Kennedy, D.R Morgan, Heat transfer and effective thermal conductivity analysis in carbon based foams for use in thermal protection systems, Proc, Inst. Mech. Eng. Part l. J Mater. Des Appl. 219(2005) 217-230.

[10] **SHENG Chen , YU Yun , YU Yang, MI Le, TANG Gen- Chu, SONG Li-Xin**, Microstructure and Thermal Characterisation of multilayer insulation materials Based on Silica Aerogels Vol 28 july 2013, Journal of inorganic materials.

[11] **Cunnington, G.R., Zierman, C.A, Funai, A.I., and Lindahn, A**, i Performance of multilayer insulation systems for Temperatures to 700K, Nasa CR-907, October 1967.

[12] **Keller, K., Hoffman, M.,Zorner, W, and Blumenberg, J.**, Application of High Temperature Multilayer Insulations, Acta Astronautica, Vol 26, No. 1992, pp.451-458.

APPENDICES

Bottom surface temperature with varying emissivity for alumina.

TIME(S)	TEMPERATURE(K)		
	.02	.05	.08
0	293.04	293.042	293.043
125	293.4	293.391	293.338
250	296.82	296.605	296.177
375	307.58	306.31	305.002
500	327.85	323.408	320.132
625	359.53	349.047	342.427
750	399.19	378.994	366.37
875	438.65	406.128	387.162
1000	472.3	426.746	402.673
1125	498.91	440.919	412.802
1250	518.41	450.870	420.251
1375	532.19	455.8	425.243
1500	542.14	462.169	428.355
1625	548.49	464.443	429.919
1750	552.57	465.946	430.6
1875	555.2	466.546	430.167
2000	555.9	466.073	427.094
2125	552.35	462.754	422.253
2250	545.92	457.429	420.124
2375	537.53	451.284	417.012
2400	535.59	449.881	415.811

Bottom surface temperature with varying density

TIME(s)	TEMPERATURE(K)		
	Density-220(Kg/m^3)	140 Kg/m^3	70Kg/m^3
0	293.04	293.512	293.619
125	293.4	294.268	297.27
250	296.82	302.253	318.526
375	307.58	324.429	360.048
500	327.85	359.458	415.766
625	359.53	459.763	479.764
750	399.19	497.061	525.511
875	438.65	524.055	548.088
1000	472.3	540.374	550.024
1125	498.91	550.795	563.133
1250	518.41	556.944	565.129
1375	532.19	560.28	564.647
1500	542.14	5610360	563.032
1625	548.49	561.407	561.841
1750	552.57	560.878	560.235
1875	555.2	558.142	555.741
2000	555.9	549.412	538.486
2125	552.35	538.471	526.186
2250	545.92	538.471	517.26
2375	537.53	527.36	511.08
2240	535.59	529.226	507.004

Bottom surface temperature by varying conductivity

TIME(s)	TEMPERTURE(K)		
	CONDUCTIVITY-0.03W/MK	28 W/MK	0.003 W/mK
0	293.04	334.656	293.001
125	293.4	405.122	293.004
250	296.82	593.928	293.018
375	307.58	548.518	293.044
500	327.85	1122.17	293.087
625	359.53	1245.08	293.142
750	399.19	1240.17	293.211
875	438.65	1235	293.309
1000	472.3	1230	293.45
1125	498.91	1224.93	293.66
1250	518.41	1210.11	293.956
1375	532.19	1199.49	294.372
1500	542.14	1171.26	294.92
1625	548.49	1169.02	295.634
1750	552.57	1157.92	296.5
1875	555.2	1095.42	297.53
2000	555.9	456.318	298.715
2125	552.35	469.955	300.693
2250	545.92	967.886	300.471
2375	537.53	600.837	302.998
2240	535.59	562.118	303.311

Bottom surface temperature when the spacer material is aerogel

TIME(s)	TEMPERATURE(K)	
	ALUMINA	SILICA
0	293.04	293.031
125	293.4	293.161
250	296.82	294.195
375	307.58	297.319
500	327.85	302.728
625	359.53	310.455
750	399.19	318.547
875	438.65	325.138
1000	472.3	330.076
1125	498.91	333.773
1250	518.41	336.556
1375	532.19	338.336
1500	542.14	339.441
1625	548.49	340.034
1750	552.57	340.392
1875	555.2	340.599
2000	555.9	340.572
2125	552.35	339.814
2250	545.92	338.458
2375	537.53	336.909
2240	535.59	336.551